Politecnico di Torino

Master's Degree in Energy and Nuclear Engineering
A.a. 2023/2024
March 2024

Uranium nitride synthesis by gas/gas reaction of UF_6 and NH_3

Master Thesis Report

Supervisors:
Raffaella TESTONI
Mikael JOLKKONEN

Candidate:
Serena AMBROSINO

Abstract

This thesis project aims to develop an innovative technique for the production of high-purity uranium nitride (UN) through the ammonolysis of fluorides. The desired objective is to perform a controlled gas/gas reaction between uranium hexafluoride (UF_6) and ammonia (NH_3) at 800°C. The intermediate product thereby obtained (uranium dinitride, UN_2) is subjected to further heating up to 1100°C under argon atmosphere, to ultimately produce UN. An inherent challenge faced in previous experiments was related to the dissociation of ammonia, which is a limiting factor for upscaling. Therefore, in this project a new setup is invented to address this challenge and it is proved experimentally: the idea is to achieve a coaxial laminar flow of UF_6 and a carrier gas, where a central stream of the former is shielded by the latter so that the two reacting gasses mix only in the hot point of the furnace, where the desired reaction can happen. To implement this approach, the ammonia dissociation has been studied, an apparatus for the controlled evaporation of UF_6 has been designed and built, and two different injection nozzles have been tested in different setup configurations. Eventually, the complete prototype has been tested altogether in a synthesis experiment at 800°C, and the products thus obtained have been converted into UN at 1100°C. Numerous auxiliary experiments have been performed using UF_4 as a reactant, as it is easier to handle and the results thus obtained can be largely extended to UF_6. Lastly, a UF_4 synthesis experiment has been performed, as educationally helpful to further dig into some chemistry features of this material, and a UN pellet has been sintered with Spark Plasma Sintering (SPS).

Keywords

Uranium nitride, synthesis, ammonolysis, uranium hexafluoride, uranium tetrafluoride, ammonia, X-ray diffraction, microscopy

Acknowledgements

I would like to express my gratitude to all those who have contributed to the realization of this thesis.

Firstly, my supervisor at KTH, Dr. Mikael Jolkkonen, for his guidance during the experiments, for sharing with me his immense expertise, for his patience and dedication to work.

I am thankful to all the people in the Nuclear Fuel Lab and in the Nuclear Science & Engineering Division, who have supported me during this journey. In particular Elina, Maria and Faris, for involving me in their exciting projects, and Fredrik, Eloi and Alejandria for being exceptional colleagues and friends. Thanks to Bosse Barksäter for his precious work in the University workshop.

I am particularly grateful to all professors at KTH and Politecnico di Torino, above all my supervisor Raffaella Testoni, for motivating and guiding me during these university years.

I would like to extend my gratitude to all the people I have encountered during my university journey, especially those who helped me to grow not only as an engineer but also as a person.

Finally, special thanks to my family for their immeasurable support and belief in my choices. And to my friends, those who are physically close to me and those who encourage me even while being far away.

Contents

1 Introduction 2

1.1 Motivations for LFRs . . . 2
1.2 Motivations for nitride fuels . . . 3
1.3 Motivations for production of UN by ammonolysis of fluorides . . . 4

2 Methods and Equipment 6

2.1 Theoretical background . . . 6
2.2 Issues to be addressed . . . 8
2.3 Equipment . . . 10
2.4 Data analysis . . . 12

3 Pressurised ammonolysis 13

3.1 Pressurised synthesis with UF_4 . . . 13
3.2 Dissociation of pressurised ammonia . . . 16

4 Pulsed-flow ammonolysis 20

4.1 Pulsed-flow experiments with argon flow . . . 20
4.2 Pulsed-flow experiments with ammonia flow . . . 23

5 Prototype for UF_6 ammonolysis 25

5.1 P-10 tubes . . . 25
5.2 Evaporation of UF_6 . . . 26
5.3 Gasses injection . . . 26
5.4 Injection tests - horizontal setup . . . 28
5.5 Injection tests - vertical setup . . . 31
5.6 Complete prototype test . . . 33
5.7 Conversion of the obtained intermediate products into UN . . . 36

6 Additional experiments 39

6.1 Synthesis of UF_4 . . . 39
6.2 ”Homemade UF_4” ammonolysis - small batch . . . 43
6.3 ”Homemade UF_4” ammonolysis - large batch . . . 46
6.4 Sintering a UN pellet . . . 49

7 Conclusions 51

References 52

Appendix 52

List of Figures

2.1 Heating systems. 10

2.2 Pressure vessel. 11

2.3 SIEMENS X-Ray Diffractometer. 12

2.4 Quantitative Gas Analyser. 12

3.1 Pressurised synthesis with UF_4 setup. 13

3.2 XRD pattern of the product of the UF_4 ammonolysis. 15

3.3 Concentration of ammonia at different pressures. 18

3.4 Relative concentrations of NH_3, H_2 and N_2 at different pressures. 19

4.1 Pulsed gas flow setup. 21

4.2 Powder comparison before and after the pulsed argon flow experiment. 22

4.3 Powder appearance after the second run of pulsed argon flow. 22

4.4 Powder appearance after the pulsed-flow run with NH_3. 24

5.1 Structure for UF_6 evaporation. 26

5.2 Structure for gasses injection and first injector design. 27

5.3 Second injector design. 27

5.4 Horizontal setup for UF_6 reaction with NH_3. 29

5.5 Product from reaction of UF_6 with NH_3 at room temperature - horizontal setup. . 30

5.6 XRD pattern of the product of the UF_6 ammonolysis in horizontal setup. 30

5.7 Vertical setup for UF_6 reaction with NH_3. 32

5.8 Product from reaction of UF_6 with NH_3 at room temperature - vertical setup. . . . 32

5.9 XRD pattern of the product of the UF_6 ammonolysis in vertical setup. 33

5.10 Product of the complete prototype test. 35

5.11 XRD pattern of the product of the complete prototype test. 35

5.12 Powder loaded in a tantalum boat. 36

5.13 Setup for the conversion of the UF_6 products into UN. 37

5.14 XRD pattern of the product of the final conversion to UN. 38

6.1 Solution of uranyl acetate and HCl. 40

6.2 Solution after addition of Zn. 40

6.3 Ultrafiltration stage. 40

6.4 Solution after addition of HF. 41

6.5 Filtration under suction. 41

6.6 Dried product in the funnel. 41

6.7 Product scraped off from the funnel. 41

6.8 Desiccation stage. 42

6.9 XRD pattern of the produced ”Homemade UF_4”. 43

6.10 UF_4 powder loaded in the copper boat. 44
6.11 ”HomemadeUF_4” small batch setup. 44
6.12 XRD pattern of the product of ”homemade UF_4” ammonolysis - small batch. . . . 45
6.13 NH_4F deposition in the quartz tube from the synthesis of ”homemade” UF_4. . . . 47
6.14 XRD pattern of the product of ”homemade UF_4” ammonolysis - large batch. . . . 48
6.15 Dr. Sinter SPS machine at the national SPS facility (Stockholm University). 49
6.16 UN pellet. 50
6.17 Sintering temperature and axial displacement for a UN pellet. 50
1 UF_6 phase diagram [4]. 54

List of Tables

2.1 Ammonolysis of fluoride reactions 8

3.1 Chemical composition of the product of the UF_4 ammonolysis* 15

3.2 Pressurised NH_3 dissociation experiment results 17

5.1 Required temperatures and voltages in the UF_6 horizontal setup 28

5.2 Chemical composition of the product of UF_6 ammonolysis in horizontal setup* . . 30

5.3 Required temperatures and voltages in the UF_6 vertical setup 31

5.4 Chemical composition of the product of UF_6 ammonolysis in vertical setup* . . . 33

5.5 Chemical composition of the product of the complete prototype test* 36

5.6 Chemical composition of the product of the final conversion to UN* 38

6.1 Chemical composition of the produced ”Homemade UF_4”* 42

6.2 Chemical composition of the product of ”homemade UF_4” ammonolysis - small batch* 46

6.3 Chemical composition of the product of ”homemade UF_4” ammonolysis - large batch* 47

6.4 Sintering parameters for a UN pellet 50

1 Physical properties of UF_6 [4]. 53

2 Physical properties of uranium compounds [3] 54

CHAPTER 1

Introduction

Concerns raised by the general public have strongly affected the development of the nuclear industry, in particular in terms of sustainability, economy, safety and non-proliferation. The Generation IV International Forum has convened the major nuclear nations to discuss a new approach for the development of the next generation of nuclear reactors. Six different reactor concepts have been selected as a focus for further research, as they have the potential to produce power in a cleaner, safer, and more efficient way. Among these, lead-cooled fast reactors (LFRs) are notably interesting and promising.

1.1 Motivations for LFRs

LFRs are fast spectrum reactors cooled by pure lead or by a eutectic mixture of lead and bismuth (LBE), operating at high temperatures and near atmospheric pressure. Lead coolants are unique among those considered for the next generation of nuclear reactors for several reasons. As a dense liquid, lead has excellent cooling properties, while its low tendency to absorb neutrons or slow them down enables LFRs to maintain a hard neutron energy spectrum with low parasitic absorption. These characteristics give LFRs an intrinsic ability to breed nuclear fuel therefore improving their sustainability and economics in terms of resource utilization, waste minimization, and extension of the core life. In the matter of safety, lead provides some unique benefits: high boiling temperature eliminates the risk of core voiding due to coolant boiling, high heat capacity provides significant thermal inertia in the event of a loss of heat sink, absence of exothermic reactions with structural materials and water avoids the formation of hydrogen and potential explosions, shield of gamma rays and retention of volatile fission products reduce the source term in case of accident. Moreover, LFRs can be designed to have a very small reactivity swing, meaning that few control assemblies are enough to compensate for the reactivity loss during operation, and the potential for reactivity insertion in case all the control rods are withdrawn is minimized. The possibility, with certain types of fuels, to design the core with greater spacing between fuel pins, leads to low pressure drop and reduces the risk of flow blockage. This, together with a simple coolant flow path and the favorable thermophysical properties of lead, enables the removal of the decay heat via natural circulation even with a very compact design, which is an advantage from the safety point of view since these reactor types can be put underground, and from the economical point of view since they are amenable to factory production. Lastly, an intermediate circuit is not needed since, due to the coolant chemical inertness, there is no need to isolate it from the steam generator. This brings a notable design simplification and it increases safety and economic performance in comparison to other Generation IV systems. Additionally, there is no degradation of the thermal cycle and a net efficiency of over 40% can be reached [1] despite the currently allowed relatively low outlet temperatures (due to limitations of structural materials).

Given all these advantages, several initiatives concerning these reactors have been started all around the world. Especially in Europe, the European Sustainable Nuclear Industrial Initiative (ESNII) has selected the LFR as a technology of interest and two main projects have been initiated: ELSY (European Lead-cooled SYstem) in 2006, to define the main options of an LFR of industrial size with a power of 1500MW$_{th}$ and 600MW$_{el}$, followed by LEADER (European Advanced Lead-cooled Reactor Demonstration) in 2010, which continued the study of an industrial-sized reactor under the name ELFR (European Lead Fast Reactor) and also initiated the concept of a demonstration LFR of power 100MW$_{el}$ called ALFRED (Advanced Lead Fast Reactor European Demonstrator). Additionally, a number of private reactor developers have started programs aiming at LFRs commercialization: Rosatom (Russia) is building BREST-300, which has the potential to be the first Gen-IV reactor, Blykalla (Sweden) is developing SEALER, NewCleo (Italy) is investing on Small-LFRs, and SCK-CEN (Belgium) intends to build an Accelerator Driven System (ADS) demonstrator called MYRRHA.

1.2 Motivations for nitride fuels

Due to corrosion/erosion of structural steels and pressure drop concerns, the velocity of lead as a coolant needs to be limited. This constitutes a peculiar disadvantage since, in order to achieve sufficient cooling, the flow area in the core needs to be quite large (i.e. the pitch between fuel rods has to be increased), causing an increase in the neutron leakage. This issue is of particular concern in the context of Generation IV reactors, as reaching a breeding ratio larger than one with oxide fuels becomes impossible without a breeding blanket. However, a solution exists with nitride fuels: uranium nitride (UN) has higher fissile density and therefore gives the possibility to successfully breed nuclear fuel, while being perfectly compatible with lead. Nitride fuels also feature a number of other properties which make them more efficient and safer than the currently used uranium dioxide fuels. They combine high melting temperature and high thermal conductivity, which increases the margin to melt and ensures a low radial temperature gradient in the fuel, in the meantime allowing to operate reactors at higher linear power. Especially interesting is that, whereas the thermal conductivity of oxide fuels is mainly dominated by lattice vibrations and decreases with the temperature, the one of nitride fuels is dominated by the electronic contribution, therefore it is much higher and increases with the temperature [2]. This property makes nitride fuels particularly attractive as ”accident-tolerant fuels”. Additionally, the high solubility of mononitrides in nitric acid makes them easily reprocessable, as the existing industrial PUREX process can be used. This is of particular interest in the context of Generation IV reactors, as it provides a solution to close the fuel cycle in fast-neutron reactors. With nitride fuels a higher burnup can also be reached, meaning that the refuelling operations can be performed more rarely, thereby providing a significant advantage from an economic point of view. On top of this, the gas release under fast reactor operating conditions is considerably lower than for oxide fuels: the latter typically range between 80 and 90%, while measured releases from nitride fuels have never exceeded 50% [2]. Low gas release means a larger probability for fission gasses to form bubbles and lead to volumetric swelling of the pellet, which increases the risk of pellet-clad mechanical interaction. However, UN fuel swelling has been studied carefully and correlations exist to predict it as a function of operating temperature and burnup, and several approaches have been tested to design the fuel rods to cope with this issue.

1.3 Motivations for production of UN by ammonolysis of fluorides

Compared to the synthesis process of oxide fuels, the uranium nitride one is more intricate. It has historically been produced by carbothermic reduction of uranium dioxide, namely streaming nitrogen over a mixture of metal oxide and carbon powder, according to the formula

$$2\,UO_2 + 4\,C + N_2 \longrightarrow 2\,UN + 4\,CO$$

The advantages of this method are the use of a widely available raw material (oxide powder) and the possibility of implementing it at a reasonably large scale. However, an issue is the presence of carbon and oxygen impurities in the final product, which are not desired especially in fast reactors, as they increase the gas release from the fuel during operation. This would require a higher gas plenum to accomodate fission gasses in the core, and therefore a bigger and more expensive design. It also seems to be excessively wasteful if the neutronically more compatible nitrogen-15 isotope is used.

A different production process investigated at KTH is the hydriding-nitriding method, through which it is possible to obtain uranium mononitride of very high purity, also using nitrogen-15. It consists of a first hydriding step where metallic uranium is exposed to hydrogen gas at a temperature of 160-250°C, according to

$$2\,U + 3\,H_2 \longrightarrow 2\,UH_3$$

a second step where the product is reacted with nitrogen at 250-500°C

$$4\,UH_3 + 3\,N_2 \longrightarrow 2\,U_2N_3 + 6\,H_2$$

and a final denitriding step at 1070-1380°C

$$2\,U_2N_3 \longrightarrow 4\,UN + 3\,N_2$$

The concern with this route is that it requires high-purity uranium metal as starting material which, at present, is not produced on an industrial scale and is not enriched for civilian purposes.

Another possibility to obtain high-purity uranium nitride is to use uranium tetrafluoride (UF_4) and uranium hexafluoride (UF_6), which are industry-standard intermediaries for the isotopic enrichment process in the production of uranium dioxide. Their ammonolysis at 800°C, in the absolute absence of oxygen, allows a very high purity of the product and has the potential to be employed in a continuous industrial process. Prior to this study, all steps of this conversion have been demonstrated individually, but many questions were still open and hardly any experiment was performed with UF_6. Therefore, the aim of this thesis project was to further investigate this route and to develop a technique which allows a controlled and upscalable production of UN powder through the reaction of UF_6 with ammonia.

Initially, some experiments have been carried out on a source of UF_4, exploring two possible solutions to the issue of ammonia dissociation, namely the pressurization of the reaction chamber (Chapter 3) and the use of a pulsed-flow of ammonia (Chapter 4). Successively, the focus was shifted to UF_6 and the challenges of a controlled gas/gas reaction have been faced (Chapter 5). Auxiliary experiments have been conducted mostly for educational purposes (Chapter 6), including the synthesis of a UF_4 batch, its reaction with ammonia, and the fabrication of a uranium nitride pellet by Spark Plasma Sintering.

CHAPTER 2

Methods and Equipment

2.1 Theoretical background

2.1.1 The chemistry of uranium compounds

Uranium can assume many chemical forms: in nature as well as in most nuclear fuel it is generally found as an oxide, fluorine compounds (mainly UF_4 and UF_6) are common in uranium processing, and in its pure form it is a silver-colored metal.

The most common forms of uranium oxide are triuranium octaoxide (U_3O_8) and uranium dioxide (UO_2). Both are solids with low solubility in water and are relatively stable over a wide range of environmental conditions. U_3O_8 is the form most commonly found in nature, while UO_2 is most commonly used as a nuclear fuel. At ambient temperatures, UO_2 gradually converts to U_3O_8. Because of their stability, uranium oxides are generally the preferred form for storage or disposal.

Uranium metal is a silver, heavy, ductile solid, with very high density (19 g/cm^3). It is not very stable, as it is subject to surface oxidation: at room temperature in air, it forms an oxide film, which prevents further oxidation of the solid. Water attacks uranium metal slowly at room temperature and rapidly at higher temperatures. Uranium metal powder ignites spontaneously in air at ambient temperature. It melts at 1132°C [3].

Uranium tetrafluoride (UF_4) is a green crystalline solid that melts at 960°C and is very slightly soluble in water. It is generally an intermediate in the conversion of UF_6 to either uranium oxides or uranium metal. It is non-volatile, non-hygroscopic, but less stable than uranium oxides. After exposure to water, UF_4 slowly dissolves and undergoes hydrolysis, forming UO_2 and hydrogen fluoride (HF), which is very corrosive. The bulk density of UF_4 varies from about 2.0 g/cm^3 to about 4.5 g/cm^3 depending on the production process and the properties of the starting uranium compounds [3].

Uranium hexafluoride (UF_6) is the chemical form of uranium that is used during the uranium enrichment process, for mainly two reasons:

- it can be used as a gas for processing, as a liquid for feeding and withdrawing, and as a solid for storage (and each of these states is achievable at relatively low

pressures and temperatures),
- because fluorine has only one natural isotope, all the isotopic separative capacity of the diffusion plant is used to enrich the concentration of the lighter uranium isotopes [4].

However, it is known that handling UF_6 is not an easy task and in order to do it safely, it is a good practice to study its chemical and physical properties. As a solid, UF_6 is crystalline and white, as a gas it is colorless. The liquid phase is not stable at atmospheric pressure. Both gaseous UF_6 and the exposed surface of the solid react rapidly with water vapor, releasing large amounts of heat (see Appendix). When gaseous UF_6 reacts with water vapor at room temperature, a white $HF - H_2O$ mist is produced, which is harmful if breathed. UF_6 also reacts with most metals to form a fluoride of the metal and a poorly volatile or non-volatile uranium fluoride. It also reacts rapidly with hydrocarbons: if in the gas phase, the reaction forms a black residue of uranium-carbon compounds, whereas if in the liquid phase, the reaction proceeds at an accelerated rate and may cause explosions. When UF_6 is processed in leak-tight piping and containers, it is not visible so it is necessary to follow its presence by observing changes in pressures or weights. Such changes are illustrated through a phase diagram (see Appendix) that shows the physical state as a function of pressure and temperature. In the experiments carried out in this thesis, particular attention was put on the transition of UF_6 from the solid to the gaseous state. According to the phase diagram, the triple point of UF_6 occurs at 1.52 bar and 64.1°C [4]: below it, solid UF_6 sublimes to gas, and gaseous UF_6 desublimes to solid; above it, liquid UF_6 vaporizes to gas, and gaseous UF_6 condenses to liquid. As heat is added to solid UF_6 in a closed system, the solid mass absorbs heat and some of it sublimes to gas. Sublimation continues until the triple point is reached (solid, gas, and liquid coexist). Additional heat incrementally melts the remaining solid, and when all of the solid has melted, further addition of heat increases the temperature of the liquid and causes a portion of it to vaporize to gas.

Physical properties of uranium compounds pertinent to this thesis project are summarised in the Appendix.

2.1.2 Ammonolysis of fluorides

The production of UN powder by ammonolysis of fluorides can be summarized into two reaction steps, that can be performed starting from UF_4 or UF_6:

1. the fluoride is heated up to 800°C and exposed to a stream of ammonia (NH_3),

producing uranium dinitride (UN_2) and ammonium fluoride (NH_4F);

2. uranium dinitride is heated up to 1100°C under argon atmosphere to obtain the final product uranium nitride (UN).

The balanced reactions involved in this process are summarised in Table 2.1.

Table 2.1: Ammonolysis of fluoride reactions

$UF_6 + 8\,NH_3 \xrightarrow{800\,^\circ\mathrm{C}} UN_2 + 6\,NH_4F$	$UF_4 + 6\,NH_3 \xrightarrow{800\,^\circ\mathrm{C}} UN_2 + 4\,NH_4F + H_2$
$UN_2 \xrightarrow{1100\,^\circ\mathrm{C}} UN + \frac{1}{2}N_2$	$UN_2 \xrightarrow{1100\,^\circ\mathrm{C}} UN + \frac{1}{2}N_2$

Both have been demonstrated experimentally, but only on a small scale. The purpose of this thesis project is therefore to propose a way to upscale the process, especially focusing on the UF_6 reactions. It was also formerly proved that the production of UN_2 is very little at any temperature below 700°C [5], therefore there is no reason to have a slow increase in the temperature of the reaction chamber, whereas a maximum yield can be obtained with a long plateau at 800°C.

2.2 Issues to be addressed

2.2.1 Ammonia dissociation

UN_2 acts as a catalyst and dissociates ammonia in a parasitic process, strongly reducing the yield of the synthesis and therefore constituting a big problem for upscaling. For solid-gas reactions, once the uranium fluoride source has reacted on the surface, and UN_2 is produced, this does not allow ammonia to penetrate further in the source. As UN_2 is the desired reaction product in the first stage, it cannot be excluded from the process, so a method is needed to

- either suppress NH_3 dissociation, or
- to enable NH_3 to very rapidly reach the unreacted fluoride.

In order to suppress NH_3 dissociation, the idea is to take advantage of the fact that the reaction $2\,NH_3 \longleftrightarrow N_2 + 3\,H_2$ is reversible at ca. 150 bar and 500°C. The required pressure is beyond what can be reached in a laboratory but would be excellent for the production of UN on an industrial scale. However, since high NH_3 pressure also allows to lower the reaction temperature (thanks to higher NH_3 activity), which reduces the dissociation rate, this line of reasoning was further investigated by building a pressurized reaction vessel to operate the synthesis at 8 bar. A synthesis experiment with this method was performed during this thesis project (Chapter 3), and the results indicated partial success.

On the other hand, a mechanism for pulsed flow was designed to deliver bursts of NH_3, aiming at mixing the powder and rapidly bringing the fresh reactant in contact with the fluoride. It was earlier proved that, at room temperature, the method was working perfectly and NH_3 could reach every part of the source. However, problems were arising during the actual synthesis experiments performed inside the furnace: the hypothesis was that the UF_4 powder was turning sticky at high temperature but, due to the lack of possibility to visually observe the powder behavior inside the furnace, this could not be proved. Therefore, a different setup was designed during this thesis project, and surprising results were collected (Chapter 4).

Another method to mechanically mix the fluoride powder by means of a rotating vessel had also been tested [5] but, since the product was still mostly caked UF_4, it was not further investigated.

2.2.2 Handling of UF_6

It is noted that the ammonolysis of uranium fluorides is accompanied by the production of hydrogen fluoride (HF) gas, which is toxic when inhaled or in contact with moist skin. In the experiments, this hazard was mitigated by performing them under ammonia atmosphere, which combines with HF to form ammonium fluoride (NH_4F), which is less hazardous and solidifies at 150°C, so can be collected at any cool point of the systems. Nevertheless, significant levels of free HF could be expected in the heated parts of the apparatus, so all operations were performed in a well-ventilated fume hood.

Generally speaking, nickel is the most suitable material to handle UF_6, followed by copper [6] and the respective alloys. Iron and its alloys vary in resistance to quite a degree, but are all inferior to copper. Ordinary glass is attacked by UF_6 in the presence of a small amount of water or hydrogen fluoride. However, in absence of these, it can be used when it is desirable to see any possible reaction, and at low pressures. On the other hand, copper has to be used when the presence of glass is undesirable or when the reactions are carried out at higher pressure [6]. Further discussion about the materials' compatibility in the experimental conditions can be found in Chapter 5.

2.2.3 Oxidation

Uranium nitrides are very sensitive to oxidation, therefore several measures were taken during the experiments to keep the highest possible purity of the products: UN and UN_2 samples were retrieved in leak-tight containers and treated inside the glove box, a flow of argon was sometimes used during assembling/disassembling procedures to avoid air intake in the reaction apparatus, a copper or tantalum lining was used inside the quartz tube to avoid the release of oxygen through the reaction

$$\mathrm{SiO_2 + 4\,HF \longrightarrow SiF_4 + 2\,H_2O}$$

and copper or tantalum shavings were used at the reaction chamber extremities to shield from convection of gasses from the outside of it.

2.3 Equipment

2.3.1 Heating equipment

Three different heating systems have been used:

- the Borel Swiss small crucible furnace KP 1100, when pressurization of the reaction chamber was adopted as a means to reduce NH_3 dissociation (Figure 2.1a);
- the Nabertherm RT 50-250/13 tube furnace, when the synthesis was performed inside the quartz tube, with horizontal and vertical setup allowed (Figure 2.1b);
- electrical heating wires and cables, wrapped around different tubes (Figure 2.1c).

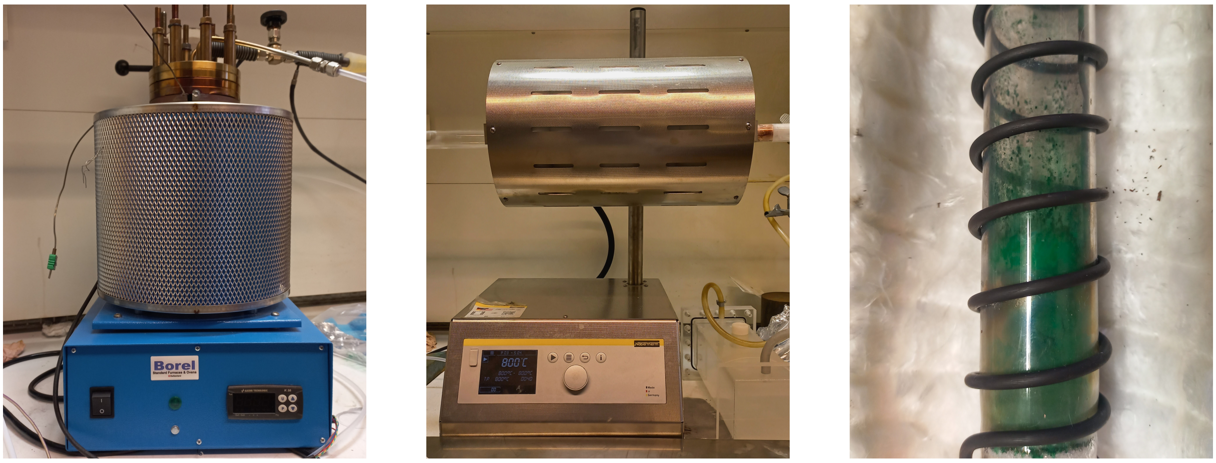

(a) Borel crucible furnace. (b) Nabertherm tube furnace. (c) Heating wires.

Figure 2.1: Heating systems.

The Borel Swiss crucible furnace also allowed larger batches of raw material with respect to the Nabertherm tube furnace. The heating wires solution was of particular interest when aiming at visualization inside the reaction chamber. Glass fibers or carbon-felt insulations were frequently used to achieve strong and uniform heat.

2.3.2 Pressure vessel

A pressurised reaction vessel (Figure 2.2) was built in the University workshop to perform the UN synthesis at NH_3 pressures up to 10 bar. The outlet was a stainless steel tube, heated by heating coils to avoid ammonium fluoride blockages, and included a valve for pressure regulation. Since Fe, Ni and Cr catalyze the dissociation of ammonia, the inner stainless steel vessel surface in contact with the gas was minimised by inserting a tantalum lining. The sample was loaded inside the vessel in a tantalum basket.

Figure 2.2: Pressure vessel.

2.3.3 Exhaust scrubbing system

A two-stage scrubbing system was used to retain any residual HF and any unconsumed NH_3 still present in the exhaust gas, taking advantage of their exceptional solubility in water. The system was constructed on purpose in the University workshop and consisted of two Plexiglas boxes:

- the first box was filled with a liquid solution of water and calcium chloride ($CaCl_2$) up to a certain level;
- the second one contained a bed of vermiculite, soaked with the same solution before every experiment run.

2.4 Data analysis

The quality of the products of the synthesis experiments was analysed using X-Ray Diffraction, as it is an accurate method to detect the composition of a powder made of elements with high atomic number. To investigate the gas composition during the studies on the NH_3 dissociation, instead, a Quantitative Gas Analyser was used.

2.4.1 X-Ray Diffraction (XRD)

The machine used was the SIEMENS D5000 X-ray Diffractometer in the Hultgren laboratory at KTH, with a $Cu_{k-\alpha}$ source (Figure 2.3). The angle was varied from 10° to 90° with 0.02° steps and the sampling time was 2 s/step. The output files were extracted in .raw format and analysed with the open-source PROFEX software [7]. The loading/unloading of the sample was performed in the glove box under argon atmosphere, and a Bruker Model A100B138-B141 specimen holder was used to provide high resolution and inert atmosphere.

2.4.2 Quantitative Gas Analyser (QGA)

The HIDEN Analytical Quantitative Gas Analyser (Figure 2.4) is a mass spectrometer configured for continuous real-time multi-species analysis of gasses [8]. It operates in vacuum and has two detectors: a Faraday cage (more accurate for high concentrations) and a semiconductor (more accurate for low concentrations). The former was chosen for this study. The exhaust gas was sampled every 2 seconds and the data was initially processed on the software directly connected to the machine and later in Matlab.

Figure 2.3: SIEMENS X-Ray Diffractometer.

Figure 2.4: Quantitative Gas Analyser.

CHAPTER 3

Pressurised ammonolysis

As mentioned in Section 2.2.1, one possible route to pursue in order to avoid the dissociation of ammonia by increasing the gas pressure. In this Chapter, experiments in this line of investigation are presented: firstly, a pressurised synthesis experiment was performed (Section 3.1) and the solid product was analysed with XRD Analysis, whereas later, a second experiment (Section 3.2) was performed with the possibility to detect also the exhaust gas composition.

3.1 Pressurised synthesis with UF_4

The purpose of this first run was mainly to test the setup and analyse the composition of the solid uranium product.

3.1.1 Setup

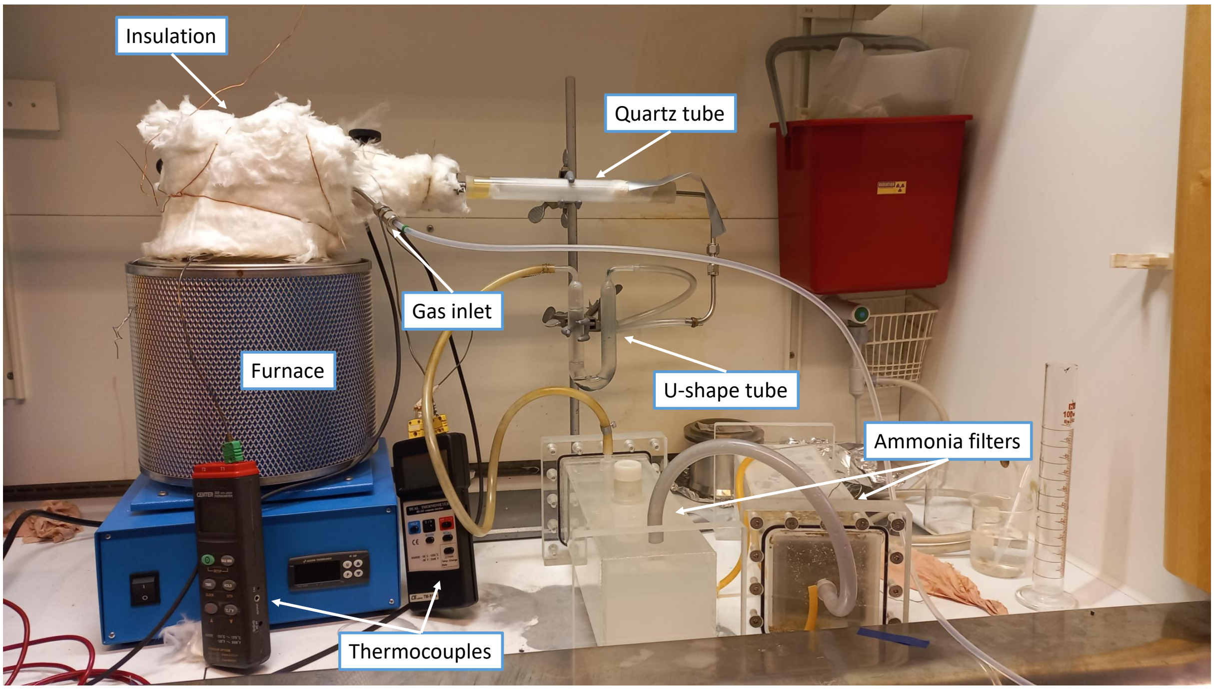

Figure 3.1: Pressurised synthesis with UF_4 setup.

The setup for this experiment is shown in Figure 3.1. The reaction was performed in the thick stainless-steel vessel (Figure 2.2), lined with tantalum to avoid ammonia contact with catalytic surfaces. Heating of the vessel was provided by the Borel Swiss crucible furnace (Figure 2.1a). The sample was positioned inside the vessel in a tantalum basket and its initial composition was 84% UF_4, 13% UO_2, 3% UN_2. An inlet hose allowed the introduction of gas inside the vessel: initially, it was connected to the laboratory circuit providing argon, while later to a tank containing pressurized ammonia. The outlet was a stainless-steel pipe, with a valve for flow regulation. This line was heated by electrical heaters, whose required voltage had been evaluated beforehand and resulted to be around 35-40V (in order to achieve at least 150°C and avoid NH_4F blockages). A quartz tube was installed for the ammonium fluoride collection, with a rubber stopper at the end, and its outlet was connected to a U-shaped bubble tube and further down to the two filters for ammonia absorption described in Section 2.3.3. The top of the furnace and the outlet tube were wrapped with glass fiber insulating material.

3.1.2 Procedure

The experiment was started with a flow of argon, 40 V on the power supply for the outlet heaters and 300°C as furnace temperature. When the vessel temperature had reached 200°C, the gas was switched to ammonia and the pressure was increased to 5 bar. Pressure and furnace temperature were further increased, up to 8 bar and 800°C. Particular attention was kept to the flow of ammonia in the U-shaped tube since it had to be large enough to replace the dissociated ammonia with fresh one. After two hours, the pressure was decreased again, switching the gas to argon at 2 bar. After cooling down for one night, the vessel was opened in the glove box and a sample was prepared for XRD analysis.

3.1.3 Results

When the furnace temperature was around 620°C, the first signs of ammonium fluoride were noticed, as white opacity in the quartz tube. Its amount at the end of the experiment was very limited, reflecting a low reaction yield (ammonia was still dissociating almost completely inside the vessel or along the outlet tube). Useful hints for the following experiments were obtained in this run:

- the vessel had reached a temperature that was much higher than the one indicated by the furnace (probably close to 860°C), due to its large thermal inertia;
- the tantalum lining used to avoid ammonia dissociation inside the vessel did not resist the conditions of the experiment;
- the powder obtained as a product was mostly black but still contained some green lumps, made of unreacted UF_4;
- some powder can be transported by the flow of gas and cause a blockage in the

valve positioned on the outlet tube.

The results of the XRD analysis of the sample are presented in Figure 3.2 and Table 3.1. Several compounds can be fit to the observed XRD pattern, notably 8.3 % UN, presumably due to the unexpectedly high temperature reached, and 22.8 % UF_4 of a crystal structure usually associated with the hydrated form. 27.3 % UF_4 was left unreacted. Peaks at 2θ = 26.9° and 2θ = 27.7° remained unidentified, probably due to the emergence of a UNx phase of intermediate stoichiometry not covered by the available crystallographic data.

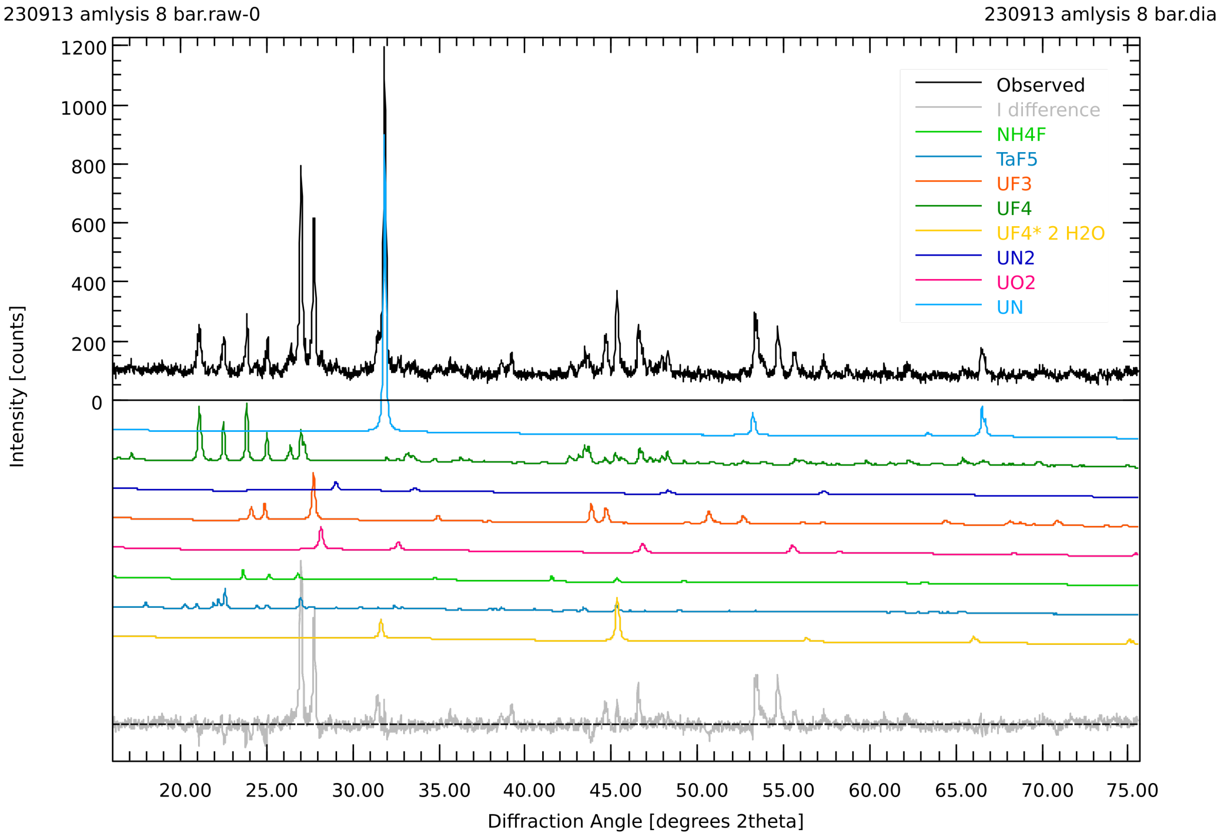

Figure 3.2: XRD pattern of the product of the UF_4 ammonolysis.

Table 3.1: Chemical composition of the product of the UF_4 ammonolysis*

UF_4	$UF_4 \cdot 2\,H_2O$	NH_4F	UF_3	TaF_5	UN	UO_2	UN_2
27.3 %	22.8 %	15.6 %	10.3 %	9.9 %	8.3 %	4.3 %	1.6 %

*Phase quantities as reported by the XRD Profex software, the accuracy is low due to counting noise [9].

3.2 Dissociation of pressurised ammonia

The aim of this experiment was to look at the dissociation of ammonia at different pressures. As discussed in Section 2.2.1, some surfaces inside the reaction vessel catalyze the dissociation of ammonia into hydrogen and nitrogen, therefore reducing the reaction yield. In order to prevent this, it would be ideal to pressurise the vessel to 150 bar, so that the reaction equilibrium is completely shifted to the formation of NH_3. This was not possible with the current laboratory setup, but it was still interesting to qualify the influence of the pressure increase.

3.2.1 Setup

The setup was very similar to the one for the synthesis experiment (see Section 3.1.1), with only two main differences:

- the QGA machine (Section 2.4.2) was connected at the outlet of the vessel, right after the valve, to detect the gas composition;
- a rotameter was connected downstream of it, in order to monitor the gas flow.

K-type thermocouples were used to measure the temperature of the vessel inside the furnace and of its seal.

3.2.2 Procedure

The flow of ammonia was started and the vessel was heated up to 635°C (temperature indicated by the furnace thermocouple). By looking at the rotameter, or at the bubbling in the U-shape tube, the flow of ammonia was monitored: the intention was to keep it as constant as possible, in order to have comparable results at the different pressures (with larger flow rate, in fact, the ammonia would spend less time inside the vessel, therefore having less time to dissociate). Initially, the gas pressure was set to 1 bar and a few minutes were waited until stable temperatures were reached. On the software connected to the QGA machine, the concentration of ammonia was observed. Then, the pressure was increased to 5 and 8 bar, always allowing the system to achieve stable conditions and observing again the concentration of ammonia at the vessel outlet. Four tests were been made. At the end of the experiment, degasification of the vessel was performed with a vacuum pump, in order to restore the properties of the tantalum contained inside, and then a constant flow of argon was injected during the cooling phase.

3.2.3 Results

Data acquired during the experiments are summarised in Table 3.2. The time in the first column is referred to the beginning of the experiment. The vessel temperature was measured by two thermocouples, therefore both values are reported in the third column. Due to the failure of the rotameter, the flow was measured through the time in which 50 bubbles occurred in the U-shape tube (a calibration was performed with a 100 ml/min flow of argon, which generated 50 bubbles in 17.64 s). Data about the concentration of ammonia are in relative percentage to the total flow of gasses detected by the QGA machine.

Table 3.2: Pressurised NH_3 dissociation experiment results

Time [h]	Pressure [bar]	Vessel T [°C]	Seal T [°C]	Flow [ml/min]	NH_3 concentration [%]
1:40	1	707/698	296	102	27
1:50	5			99	31
2:10	8			101	36
2:30	1	712/704	336	105	22
2:40	5			107	27
2:50	8			109	36
3:10	1	715/707	353	104	20
3:20	5			108	28
3:30	8			108	36
3:45	1	715/708	363	105	20
4:00	5			110	31
4:15	8			101	34

The concentration of ammonia measured by the QGA machine is also graphed in Figure 3.3, where the time spent at 1, 5 and 8 bar is highlighted in red, yellow and purple respectively. In Figure 3.4, instead, the relative concentrations of ammonia, hydrogen and nitrogen are shown: the symmetry between the NH_3 and the H_2 concentrations, as well as the fact that the concentration of H_2 is roughly three times the one of N_2, prove that the variations in the ammonia concentration are indeed due to dissociation.

Important conclusions were drawn from this experiment:

- by increasing the pressure, the concentration of undissociated ammonia at the vessel outlet indeed increases, and this was achieved consistently in all four tests, which all show very nice plateaus at the different pressures;
- there is a general tendency in the ammonia concentration to decrease over time,

probably caused by the seal heating, which increases the dissociation in the upper part of the system;

- every time the pressure is changed, the ammonia dissociation has a substantial increase, due to the larger flow introduced all of a sudden (for example, when increasing the pressure from 5 to 8 bar, three times more fresh ammonia is introduced in the system at once);
- then, the concentration generally reaches a local minimum that can be attributed to some old dissociated ammonia still residing in the system, before stabilizing at a new level (this is not experienced at 1 bar);
- during the fourth test at 5 bar, the concentration of ammonia in the graph (Figure 3.3) seems very unstable, but this can be explained in relation to the flow (all the increases in concentration were linked to increases in flow and vice versa).

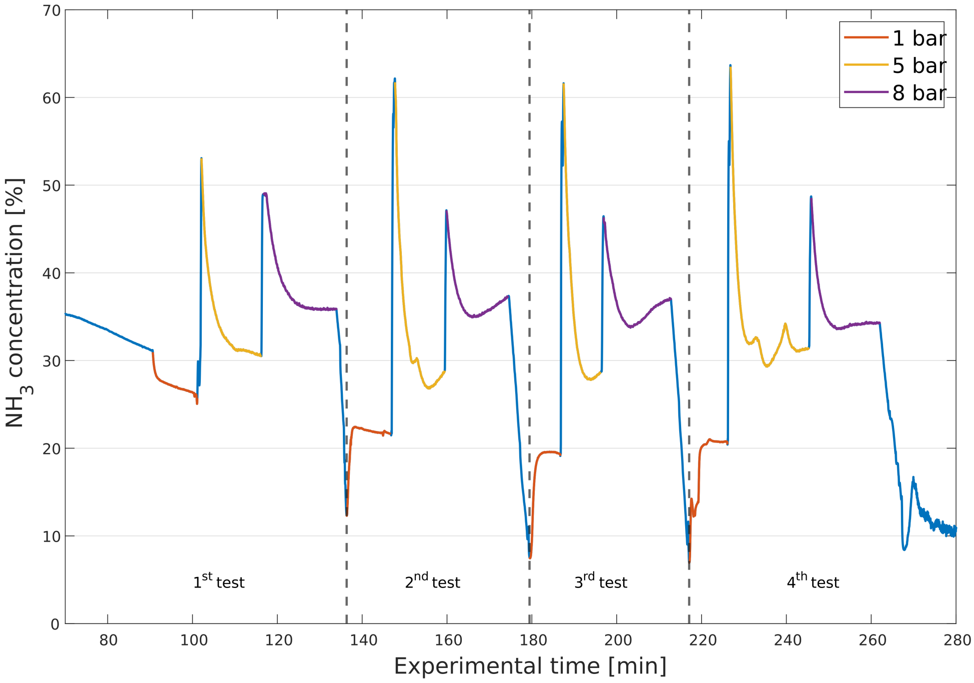

Figure 3.3: Concentration of ammonia at different pressures.

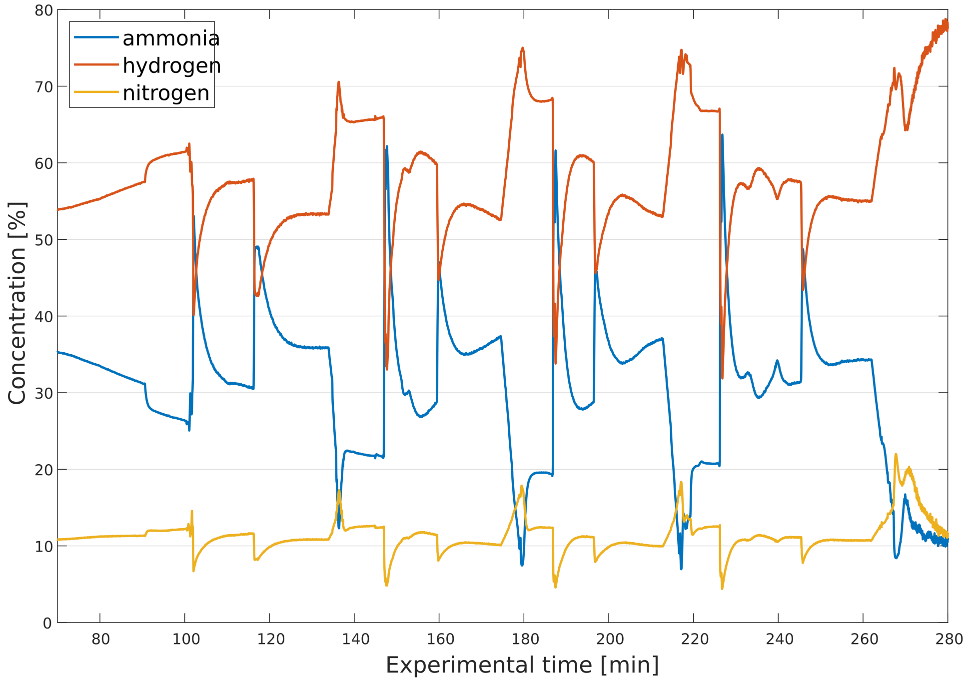

Figure 3.4: Relative concentrations of NH_3, H_2 and N_2 at different pressures.

The experiment was overall very successful, proving that an increase in the operating pressure has a strong potential to limit the dissociation of ammonia. In a normal synthesis experiment, the dissociation is generally expected to be higher, due to the presence of UN_2 but, on the other hand, in industrial applications the pressure could also be raised further. It would be of interest for further studies to repeat the experiment reaching higher pressures, to see at which level the dissociation is limited to reasonable levels.

CHAPTER 4

Pulsed-flow ammonolysis

As described in Section 2.2.1, a possible solution to suppress ammonia dissociation is to enable it to very rapidly reach the uranium fluoride powder, and at the same time mix the latter in order to expose the unreacted material to the gas flow. A setup to achieve this had been designed, with the idea of generating gas pulses that blow up the powder inside the reaction tube (jump). During this thesis project, some experiments have been performed to investigate the powder behavior in this setup configuration at different temperatures, initially in a flow of inert gas and then in ammonia. They are presented in this Chapter.

4.1 Pulsed-flow experiments with argon flow

The very first run of this experiment aimed at testing a new setup that allowed visualization of the powder during heating up to 660°C. From the previous experiments, the expectation was to observe the powder becoming sticky and caking up when increasing temperature. Since with this first run it was proved that this was not the case, a second run was performed heating up to 750°C (the temperature at which UF_4 would start to convert to UN_2 if exposed to ammonia).

4.1.1 Setup

Slightly more than 8 g of UF_4 powder were used for this experiment, deposited as a 4 mm layer on a frit inside a 25 mm ID quartz tube oriented vertically. An electronic system for gas delivery was previously constructed and delivered 9 ml of gas every 8 seconds at 4.5 bar from the bottom of the quartz tube. The pulsed controller was fed with a 24 V supplier. Two heating coils were wrapped around the quartz tube and fed with a power supply: determining which voltage was to be used on it to achieve the desired synthesis temperatures was one of the objectives of the first run. Insulating material was placed around the tube, leaving a loose part to allow an opening for visualization inside. A thermocouple was inserted inside the tube to detect the exact temperature.

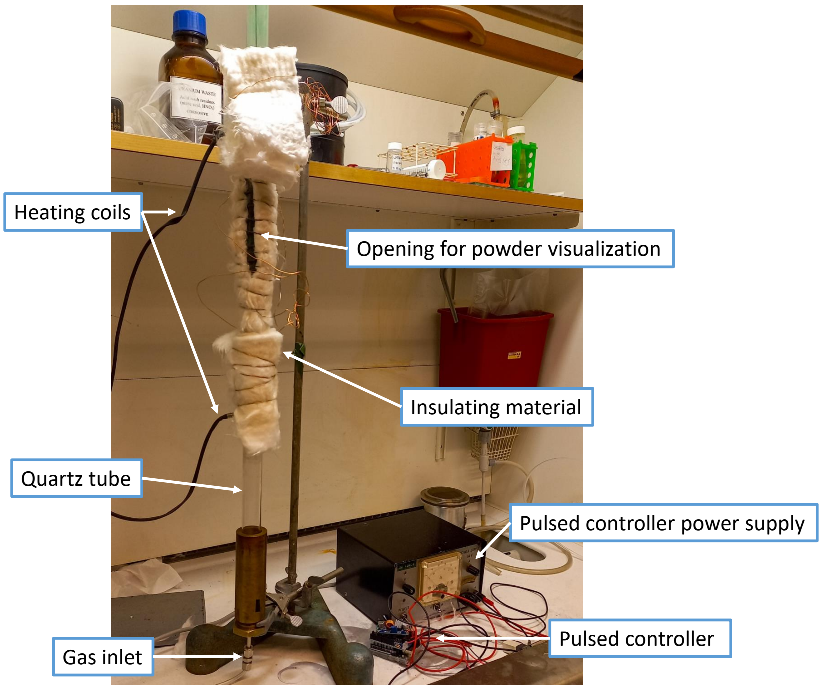

Figure 4.1: Pulsed gas flow setup.

4.1.2 Procedure

The pulsed argon flow was started, as well as the heating. The UF_4 powder started to jump from the filter pushed by the pulses and redeposited on it before jumping again. The voltage on the heaters' power supply was initially set to 60 V and then adjusted in order to keep a regular heating rate. The powder was observed at different temperatures from the opening in the insulation. Cooling was started at 660°C and 750°C in the first and second run respectively, still keeping the pulsed argon flow. The re-formed powders were studied in an optical microscope and compared with the fresh one.

4.1.3 Results - first run

The voltage on the heaters' power supply had to be increased to 70 V at 350°C, to 80 V at 460°C, to 90 V at 520°C and to 100 V at 600°C to maintain a reasonable heating ramp. At low temperatures (up to 350°C), the powder behaved like dry dust and jumped with the gas pulses, staying airborne for 4-5 seconds. At temperatures between 350 and 500°C, the powder was unexpectedly still jumping as fine dust, but an increasing amount of material was sticking on the quartz tube walls (mainly in an area 3 - 4 cm above the filter, where most of the grains were losing the upward speed and started falling back). At 600°C, the powder was not jumping as high as before and the air was clearing faster, but only at 660°C no more powder motion was observed. Even more remarkable, during cooling it was noted that the powder had started to jump again, in the same way as at the beginning of the experiment. The tube walls were also progressively cleaned up by the jumping powder. When the powder was extracted from the tube, it looked exactly as at the beginning of the experiment. More proof of this was obtained by analysing the powder in the optical microscope (Figure 4.2): no signs of liquefaction were noted and the powder kept being very granular.

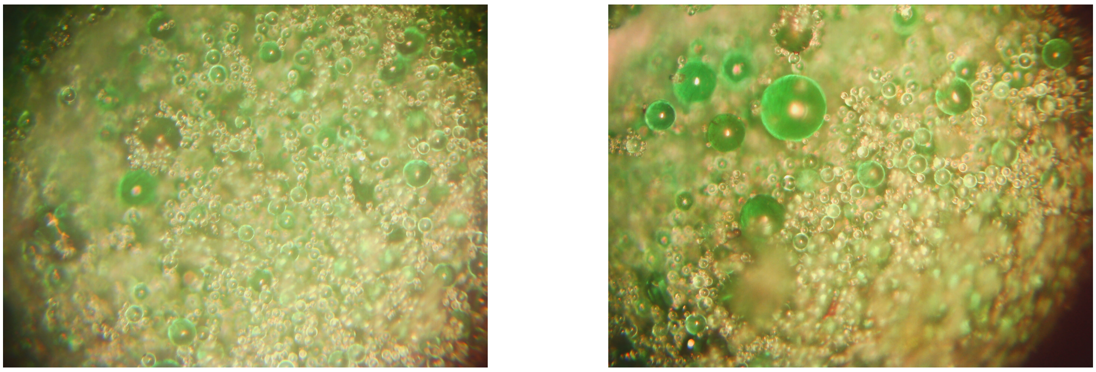
(a) Before the experiment.
(b) After the experiment.

Figure 4.2: Powder comparison before and after the pulsed argon flow experiment.

4.1.4 Results - second run

Up to 500°C, the observations were very similar to the ones in the first run, but a strong reduction in the moving powder was observed between 500 and 600°C. At 600°C, no powder was jumping anymore (note that the quantity of powder in this second run was notably smaller than in the first one). The major difference was that, around 700°C, the quartz tube started to be darker in color and opaque, not allowing any further visualization. However, when the powder was taken out from the tube, it looked once again very similar to the initial one, both at the macroscopic and microscopic scale: some of the granules seemed to have a tendency to agglomerate into bigger structures (see the right bottom corner in Figure 4.3b), but most of them were still loose.

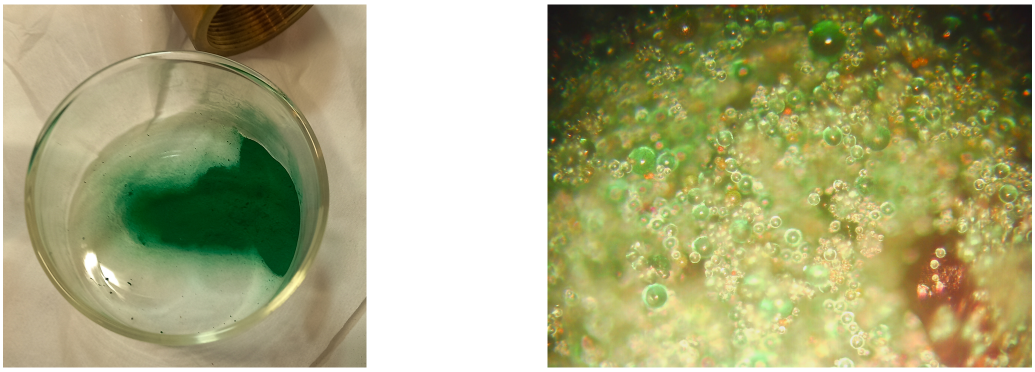
(a) Sample retrieved from the tube.
(b) Microscope image.

Figure 4.3: Powder appearance after the second run of pulsed argon flow.

In light of this, it was concluded that no ”caking” of the UF_4 powder occurs (at least not in argon): when agitated, the powder does not extensively aggregate grain-to-grain in the powder bed or form lumps, whereas it adheres to solid surfaces. Moreover, there is no partial liquefaction of grains, as no sign of this was noted, also at the microscopic level.

4.2 Pulsed-flow experiments with ammonia flow

Given the promising findings of the two runs in argon, the same setup was tested in a flow of ammonia.

4.2.1 Setup

The same setup as in the case of argon flow was used, but the temperature was kept below 700°C so that the UF_4 - NH_3 reaction could not start. As mentioned in Section 2.2.3, hydrofluoric acid (HF) produced in the ammonolysis of UF_4 can react with silica (SiO_2) producing oxygen impurities. Therefore, for a proper synthesis run at a higher temperature, all quartz components would need to be replaced. Nevertheless, one filter for NH_3 and HF absorption was used in this run.

4.2.2 Procedure

The procedure did not vary from the one used in the experiments with argon: gas flow was started and heating was provided with 60 V on the heaters’ power supply. The powder was observed at different temperatures from the opening in the insulation. The voltage had to be increased to 110 V to achieve 700°C. The re-formed powder was studied in an optical microscope.

4.2.3 Results

At the beginning of the experiment, the UF_4 powder jumped very nicely and loose under the NH_3 pulses. The powder remained green for the whole experiment and very little ammonium fluoride deposition was noted in the tube cold zone, proving that the reaction was not started. Around 650°C, the amount of jumping powder was notably decreased: most of it was stuck on the solid surfaces (the tube wall and the thermocouple) but did not show any sign of liquefaction or agglomeration at the macroscopic level. When observed in the microscope, some aggregates could be observed, as the red structure in Figure 4.4b.

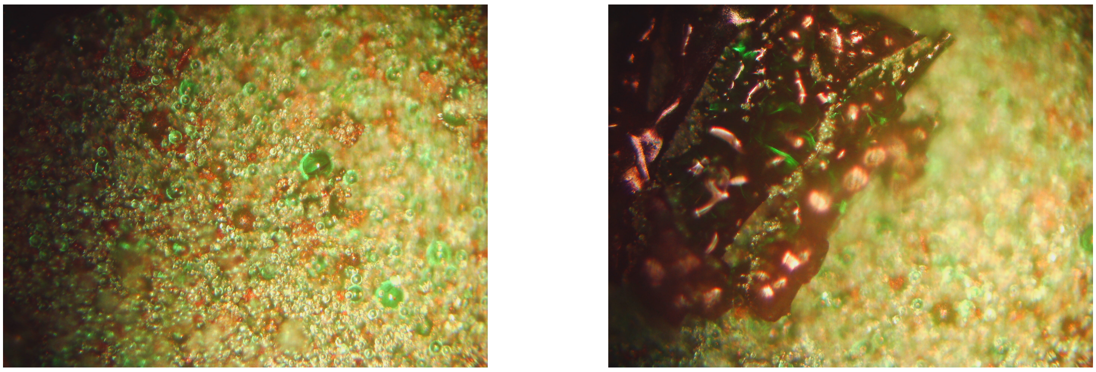

(a) General appearance.

(b) Detail.

Figure 4.4: Powder appearance after the pulsed-flow run with NH_3.

Even though the pulsed-flow route was not further investigated during this thesis project, the results obtained were very promising and some further work is encouraged. By adding a copper or tantalum lining inside the quartz tube and depositing the UF_4 powder on a steel mesh, an oxygen-free environment can be obtained, and a proper synthesis run can be performed. The drawback would be the lack of visual observation of the powder behavior, but no agglomeration is expected in the nitrided powder.

CHAPTER 5

Prototype for UF_6 ammonolysis

The radical change of UF_6 with respect to UF_4 is that the former is delivered in its gaseous phase, so the reaction with ammonia is of the gas/gas type. Before this thesis project was started, one synthesis experiment using about 4 g of UF_6 had been performed, but its setup was such that UF_6 was delivered, before the synthesis run was started, as a solid in a single load, which is not optimal in terms of reproducibility. However, its outcomes were the starting point for the investigations carried out in this thesis project [5]:

- the gas/gas reaction between UF_6 and NH_3 can successfully produce UN,
- the reaction occurs spontaneously and can become very energetic, so it is essential to moderate the reaction rate through a slow and controlled supply of UF_6 to the reaction chamber,
- the reaction is instantaneous and will cause blockage of any inlet of UF_6 vapor unless it is cleverly designed.

Suitable materials for UF_6 handling had to be chosen for this prototype: platinum and gold, the most inert materials known, are easily attacked by UF_6 at temperatures above 400°C (because, due to the volatility of their fluorides, a fresh metallic surface is continuously produced [6]). Therefore, for high-temperature applications, metals producing non-volatile fluorides have to be adopted, such as nickel, copper and tantalum. Given that the first acts as a catalyst for ammonia dissociation, the latter two were chosen for the experiments.

5.1 P-10 tubes

UF_6 samples are packaged in P-10 tubes to prevent sublimation and reaction with moisture in the air. The tube is made of polychlorotrifluoroethylene (PCTFE), which is a semi-transparent thermoplastic with an extremely low water vapor transmission rate and one of the highest limiting oxygen index [10]. A PCTFE gasket covers the tube's opening, and a nut and plug (in Monel or stainless-steel) seal the gasket to the tube [11]. Their capacity is approximately 13 g of UF_6. For each experiment involving UF_6, the P-10 tube was opened inside the fume hood and quickly connected to the apparatus ready to host the reaction, in order to minimize its contact with moisture in the air and the formation of the $HF-H_2O$ compound (a white mist).

5.2 Evaporation of UF_6

An apparatus for evaporation of UF_6 from P-10 tubes was constructed in the University workshop: it consists of an inner copper structure that holds the P-10 tube and provides heating by means of heating electric wires that surround the tube plug (Figure 5.1a), and an outer stainless steel shell that encloses the electrical connections to the heaters and the two thermocouples which detect the temperatures on the tube (Figure 5.1b). Both structures have an aperture to allow us to look over the evaporation rate and the amount of UF_6 left in the tube.

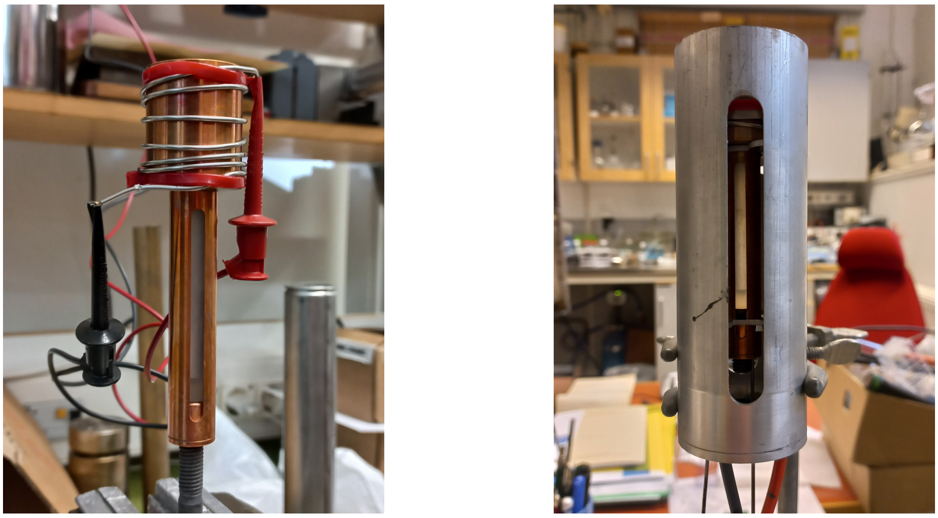

(a) Inner structure.

(b) Outer shell.

Figure 5.1: Structure for UF_6 evaporation.

At the exit of the evaporating apparatus, a stainless-steel capillary tube was used to guide the gas flow to the reaction chamber. It was enclosed into a copper tube, heated by electric heaters and wrapped into carbon felt insulation to keep the temperature above the UF_6 sublimation temperature along the whole connection (56.6°C at atmospheric pressure).

5.3 Gasses injection

The general idea for the injection of gasses was to have a central UF_6 stream shielded by a coaxial stream of inert gas, which mixed with ammonia only in the hot zone of the reaction tube. The reasoning behind this is firstly the incompatibility of hot UF_6 with any material possibly used for its injection, and secondly the possibility of separating the product (UN_2) from the fresh ammonia and avoiding the dissociation of the latter. To achieve this, the stainless steel capillary tube was inserted into a wider injection tube, along which also the inert gas was introduced, as in Figure 5.2. A rubber stopper was used to pair it with the ammonia inlet tube and to make a seal against the reaction tube.

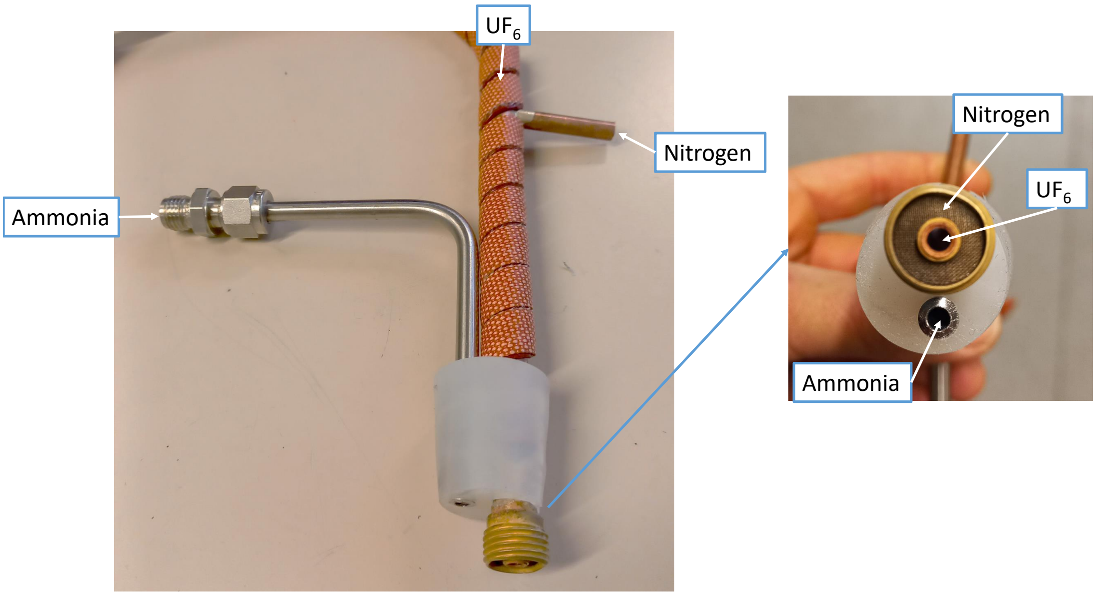

Figure 5.2: Structure for gasses injection and first injector design.

For the tip of the injection tubes, two different solutions have been tested to achieve the best possible laminar flow of gasses and to avoid backflow of ammonia through the capillary tube: the first was a gas lens from TIG welding (Figure 5.2), where the inert gas was uniformly distributed around the UF$_6$ capillary, whereas the second was a flow-guide device (Figure 5.3), where the inert gas flow was split into four channels with smaller cross-section.

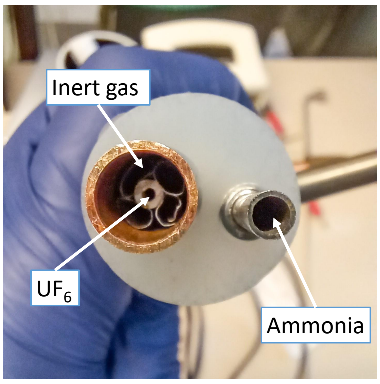

Figure 5.3: Second injector design.

Nitrogen was generally used as inert gas for mainly two reasons:

1. it does not dilute ammonia per se because, since it is one of the two products of its dissociation, it does not shift the equilibrium of the reaction towards the

dissociation itself;

2. its small molecular weight makes sure that, once injected, it will exit the reaction chamber from its top (helium would be a better candidate in this sense, but it would be worse in terms of point 1).

5.4 Injection tests - horizontal setup

This experiment aimed to prove the evaporation of UF_6 through the constructed evaporator, and the possibility to react it with NH_3 in a controlled way. Moreover, it was of interest to see the injector's behavior and test possible variations of it. The different heating systems had been tested individually beforehand, and the respective required voltages had been identified as in Table 5.1. No heating of the reaction chamber (the quartz tube) was provided, therefore the reaction of UF_6 with NH_3 was expected to result in the formation of tetravalent uranium ammonium fluorides, such as uranium ammonium pentafluoride NH_4UF_5, according to [12]

$$3\,UF_6 + 8\,NH_3 \longrightarrow 3\,NH_4UF_5 + 3\,NH_4F + N_2$$

The reaction was expected to result in a green/blue voluminous product.

Table 5.1: Required temperatures and voltages in the UF_6 horizontal setup

	Temperature range	Required voltage
UF_6 evaporator	56 / 60°C	9 / 10 V
UF_6 injection tube	> 76°C	200 V

5.4.1 Setup

The setup used for this experiment is shown in Figure 5.4: the UF_6 evaporator containing the P-10 tube was connected to the injection tube, which was wrapped into carbon felt insulation. The N_2 inlet was connected to the laboratory gas circuit, therefore its flow could be controlled precisely via software, while the NH_3 inlet was simply connected to a tank, so its flow was controlled through a U-shaped bubble tube positioned at the quartz tube outlet. The rubber stopper provided a leak-tight connection to the reaction chamber, at whose outlet side a wad of paper tissue was placed to stop any solid product from moving further with the gas flow. One ammonia filter of the type described in Section 2.3.3 was positioned at the end of the outlet tube. Several K-type thermocouples were used to check the temperatures at different spots.

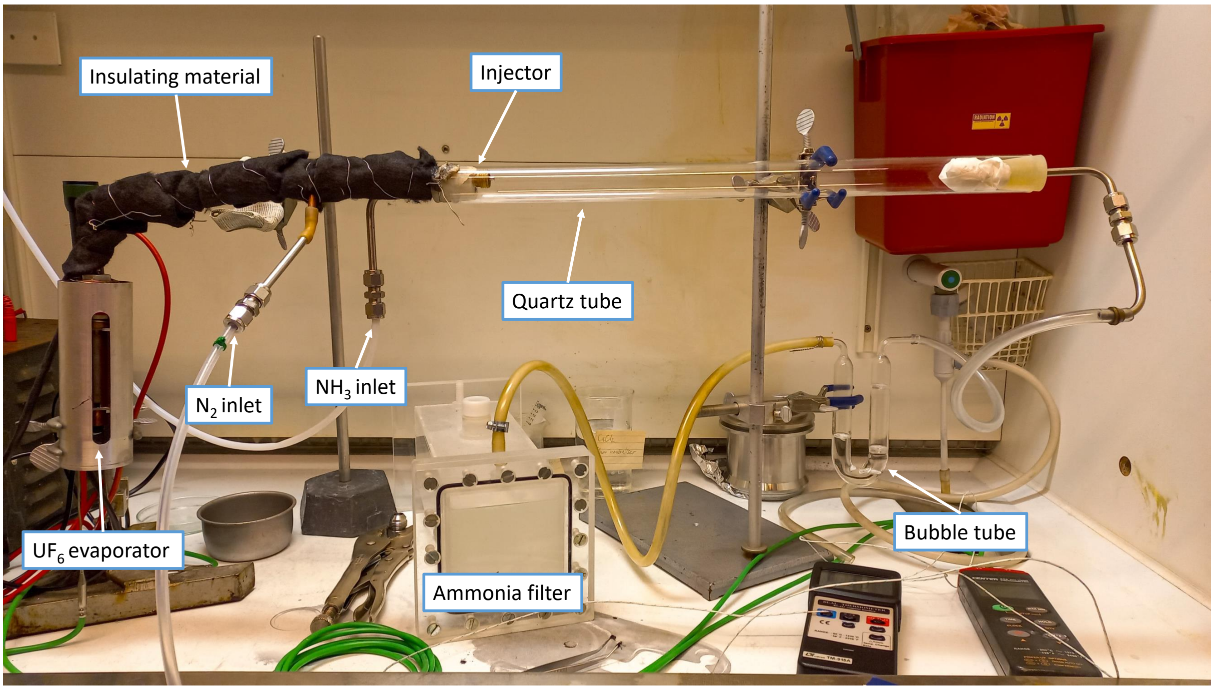

Figure 5.4: Horizontal setup for UF_6 reaction with NH_3.

5.4.2 Procedure

The procedure was the following:

1. Connect the P-10 tube to the stainless-steel capillary and place it inside the evaporator;
2. Start the N_2 flow (0.15 l/min);
3. Start heating the UF_6 injection tube;
4. Wait until the temperature in the whole tube has reached at least 76°C (~10°C margin to the sublimation temperature);
5. Start heating the UF_6 evaporator;
6. Start the NH_3 flow;
7. Let the reaction happen;
8. Switch off the evaporator heater;
9. Stop the NH_3 flow;
10. Switch off the pipe heaters and let everything cool down.

5.4.3 Results

The experiment successfully demonstrated the UF_6 evaporation and its reaction with NH_3: when the temperature on the evaporator was around 45-50°C, the first traces of NH_4F were detected inside the quartz tube as white cloudiness, starting from the left side and gradually expanding towards the right. Successively, a good amount of uranium NH_4UF_5 was also formed (green product), as shown in Figure 5.5.

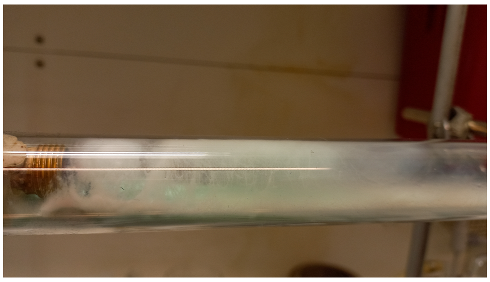

Figure 5.5: Product from reaction of UF_6 with NH_3 at room temperature - horizontal setup.

Further evidence was given by the results of the XRD analysis, which are shown in Figure 5.6 and Table 5.2. Peaks at $2\theta = 26.7°$ and $2\theta = 46.2°$ remained unidentified.

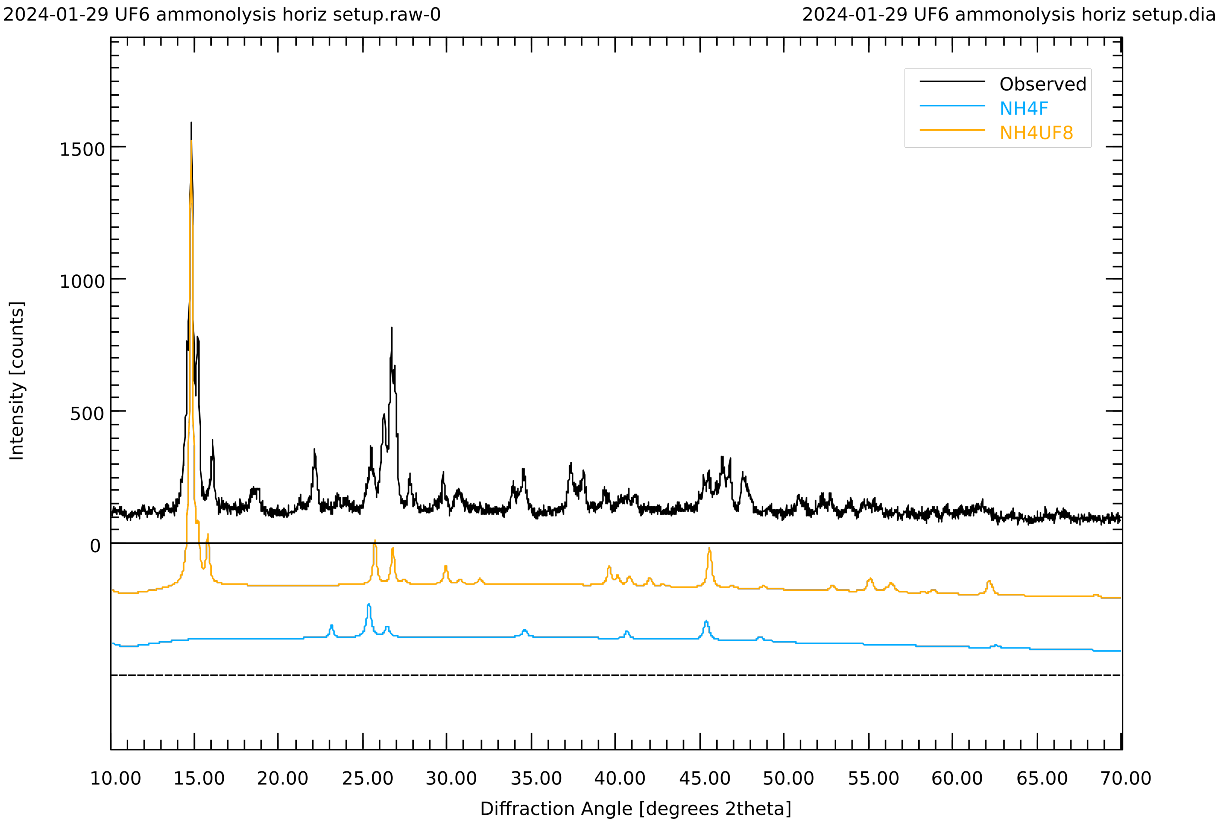

Figure 5.6: XRD pattern of the product of the UF_6 ammonolysis in horizontal setup.

Table 5.2: Chemical composition of the product of UF_6 ammonolysis in horizontal setup*

NH_4F	$(NH_4)_4UF_8$
90 %	10 %

*Phase quantities as reported by the XRD Profex software, the accuracy is low due to counting noise [9].

One issue observed during the first run of this experiment was a partial misoperation of the injector: the inert gas was not transporting UF_6 inside the reaction tube as expected, whereas the latter was reacting immediately after the injector, and the product could potentially block the capillary tube. To address this, other runs were performed with different arrangements: first, the ammonia outlet tube was extended further inside the quartz tube, then a sleeve was added to the injector to shield the UF_6-N_2 flow even better from the NH_3, and lastly a spot of grease was deposited on the capillary outlet to avoid backflow of NH_3. The combination of the three improvements seemed to have the most promising result, but still insufficient. Therefore, the new injector (Figure 5.3) was designed and later used in the complete prototype test.

5.5 Injection tests - vertical setup

As explained in Section 2.2.1, it is essential to separate the reaction product from the fresh ammonia, in order to avoid dissociation of the latter. With this experiment, the intention was to prove that the formed NH_4UF_5 could precipitate under gravity on a filter at the bottom of the reaction tube and separate from NH_4F, which was intentionally collected in a separate quartz tube (in principle, this was easily achievable by keeping the whole system at a temperature above 150°C, except for this second quartz tube, where the NH_4F was allowed to condense). Also in this case, the required heaters had been tested beforehand and the required voltages had been noted (Table 5.3).

Table 5.3: Required temperatures and voltages in the UF_6 vertical setup

	Temperature range	Required voltage
Quartz tube	~200°C	60 / 120 V
NH_3+NH_4F outlet	> 150°C	45 V

5.5.1 Setup

In order to benefit from gravity to potentially collect the product, a vertical setup was chosen, as shown in Figure 5.7: besides their orientation, evaporator, injector and reaction chamber remained unchanged, but this time the quartz tube was heated and NH_3 was injected from the bottom. The quartz tube for NH_4F collection was placed close to the upper side of the reaction chamber, and the regular filter for ammonia absorption was downstream of it.

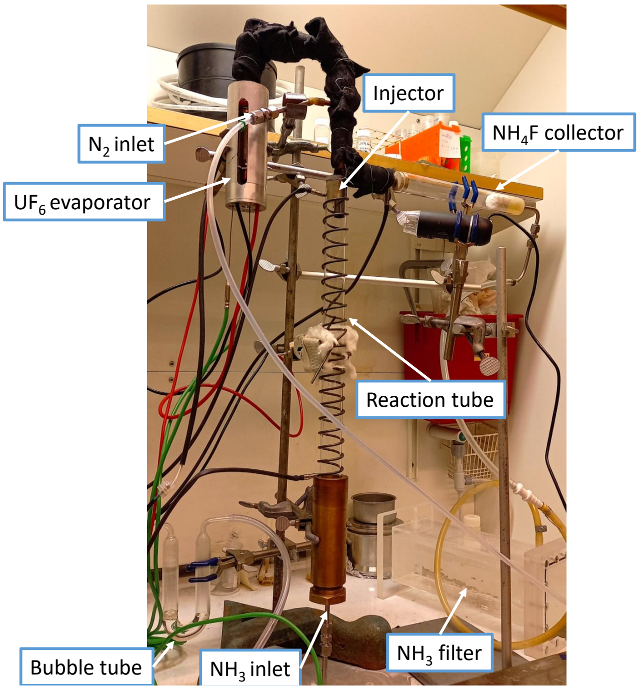

Figure 5.7: Vertical setup for UF_6 reaction with NH_3.

5.5.2 Procedure

The procedure was very similar to the one used for the horizontal setup, with the NH_3+NH_4F outlet heaters and the quartz tube heaters switched on right after the UF_6 inlet ones.

5.5.3 Results

Unfortunately, this experiment did not give the expected results: most of the uranium product did not fall on the reaction tube filter but was lifted by the stream of NH_3 and accumulated in the NH_4F collection tube, as shown in Figure 5.8.

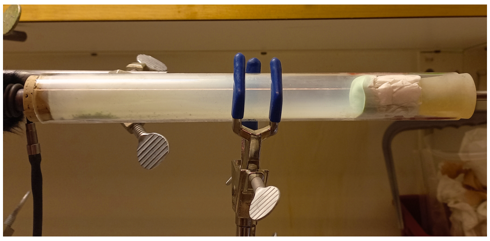

Figure 5.8: Product from reaction of UF_6 with NH_3 at room temperature - vertical setup.

The results of the XRD analysis (shown in Figure 5.9 and Table 5.4) were difficult to interpret since several different uranium-ammonium-fluoride compounds could be fit with the observed pattern.

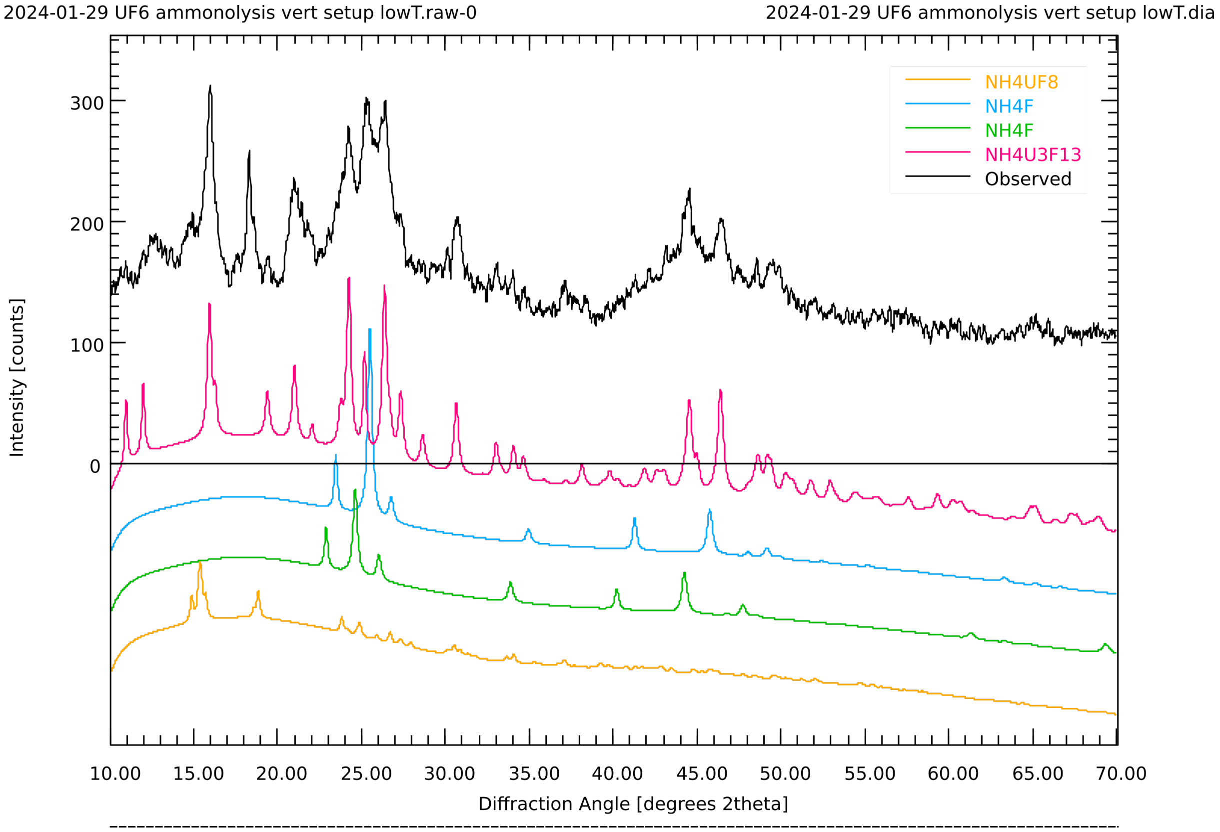

Figure 5.9: XRD pattern of the product of the UF$_6$ ammonolysis in vertical setup.

Table 5.4: Chemical composition of the product of UF$_6$ ammonolysis in vertical setup[*]

NH_4F	$NH_4U_3F_{13}$	$(NH_4)_4UF_8$
66.7 %	28.0 %	5.3 %

[*] Phase quantities as reported by the XRD Profex software, the accuracy is low due to counting noise [9].

5.6 Complete prototype test

This experiment aimed at reaching the target reaction temperature (800°C) in the reaction tube, in order to test the whole prototype in an actual reaction run.

5.6.1 Setup

The evaporator and injector parts were similar to the case described in Section 5.5.1, but a few changes were made in the reaction chamber:

- a quartz tube with glass frit in the middle was used;
- a fine steel mesh was placed on the glass frit to avoid oxidation and prevent solid particles from proceeding further;
- copper lining was used inside the quartz tube to avoid oxidation of the product;

- argon was used as inert gas, in order not to nitride the steel mesh and perhaps cause a blockage;
- the gas flows were concurrent, all injected from the top;
- the Nabertherm tube furnace (Figure 2.1b) was used to provide uniform heating of the quartz tube;
- a glass cylinder was placed at the gas outlet, to measure potential over-pressurization of the reaction chamber through a counter pillar of kerosene.

The intention was to collect NH_4F in the lower part of the quartz tube, below the furnace, which was the cold zone of the system. The upper part of the quartz tube, instead, was kept quite hot by convection of hot gas from the furnace.

5.6.2 Procedure

The procedure was the following:

1. Connect the P-10 tube to the stainless-steel capillary and place it inside the evaporator;
2. Expel the air inside the system by injecting argon (0.15 l/min);
3. Start heating the UF_6 injection tube;
4. Wait until the temperature in the whole tube has reached at least 76°C;
5. Start heating the furnace (20°C/min ramp);
6. Start heating the UF_6 evaporator;
7. Start the NH_3 flow when the evaporator has reached 35°C;
8. Let the reaction happen;
9. Switch off the evaporator heater;
10. Stop the Ar flow and leave the NH_3, in order to nitride the product completely;
11. Stop the NH_3 flow;
12. Switch off the pipe heaters and let everything cool down in a flow of Ar.

5.6.3 Results

Overall, the experiment was successful, but it also pointed out some weak points of the setup, which need further improvement. Firstly, the steel mesh well collected the solid product of the reaction, but this quickly clogged the mesh pores and therefore the pressure in the reaction chamber started to increase. To solve this problem, a different arrangement to collect the product has to be designed, in which large quantities of powder can accumulate. Extracted from the reaction tube, the mesh presented as in Figure 5.10.

Figure 5.10: Product of the complete prototype test.

The major issue detected was the insufficiency of the copper lining to avoid oxidation: during this experiment, it was placed only in the hot zone of the furnace but some water could still form from the reaction of hydrofluoric acid (HF) with quartz in some other parts of the reaction chamber. Unfortunately, this led to the oxidation of the product: the XRD analysis showed a perfect UO_2 pattern, as shown in Figure 5.11 and Table 5.5, with almost no traces of UN.

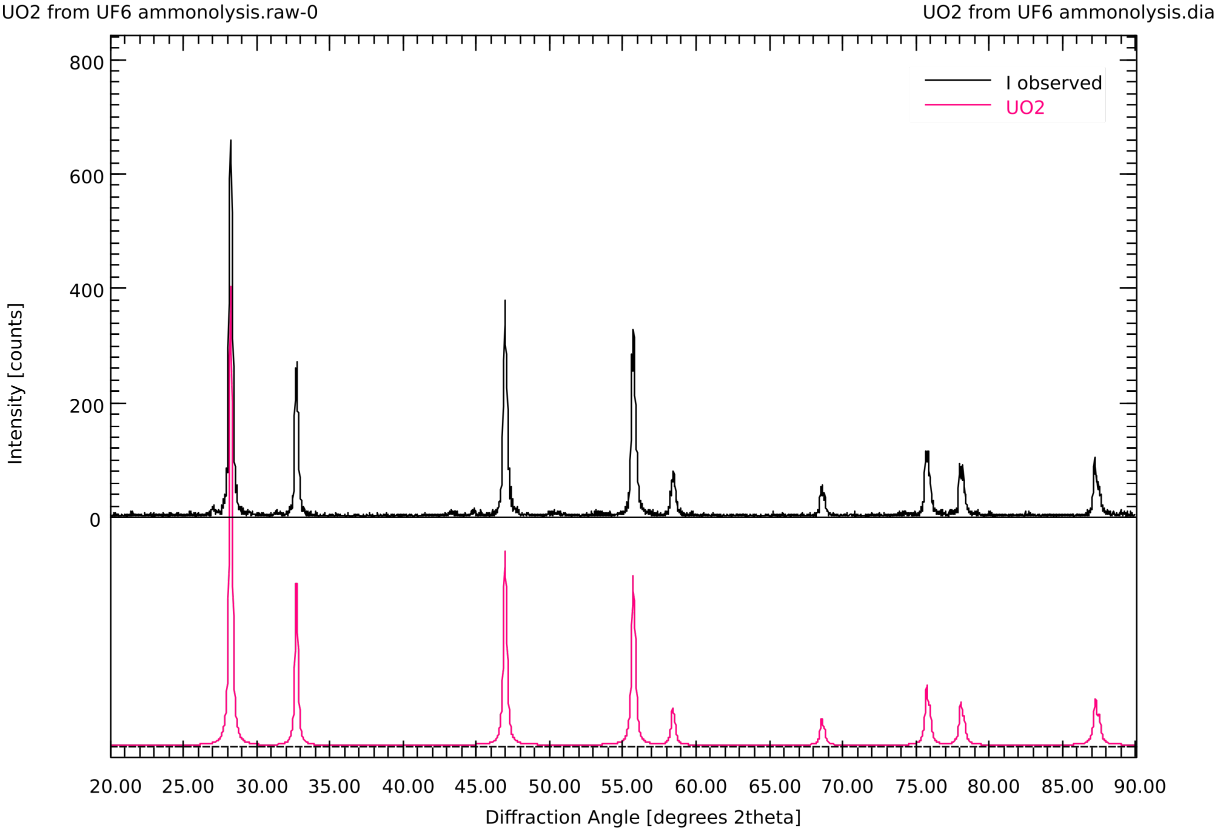

Figure 5.11: XRD pattern of the product of the complete prototype test.

Table 5.5: Chemical composition of the product of the complete prototype test*

UO_2	UF_4	UN_2	UN
99.44 %	0.46 %	0.00 %	0.10 %

*Phase quantities as reported by the XRD Profex software, the accuracy is low due to counting noise [9].

This was indeed an extraordinary result: it proved that the gas/gas reaction between UF_6 and NH_3 can successfully evolve in a controlled manner, and the uranium product can be collected separately from the gaseous products. With a fully oxygen-free setup, this technique can effectively produce UN_2 and eventually UN.

5.7 Conversion of the obtained intermediate products into UN

In this part of the work, the aim was to convert the various products obtained by UF_6 ammonolysis into uranium mononitride (UN). This procedure was well-known and had been successfully done prior to this thesis project, but only on the product of a solid-solid reaction, which had a different morphology to the ones hereby obtained. It was noteworthy that the powders, which initially appeared mostly white, had with time turned more toward a green color, as presented in Figure 5.12.

Figure 5.12: Powder loaded in a tantalum boat.

5.7.1 Setup

The major difference of this run as compared to the previous ones was the target temperature, namely 1100°C. Copper could not be used (its melting point is 1085°C), therefore tantalum had to be chosen. The sample was loaded in an 11 cm tantalum magnetically retractable boat inside a quartz tube (1 m length, 25 mm ID, 28 mm OD) oriented horizontally. The tube was inserted inside the Nabertherm furnace and it was held at both ends by brass fittings. Tantalum lining was used in the hot zone to avoid the reaction of hydrogen fluoride (HF) with the quartz, and tantalum shavings were used at the furnace edges to shield the sample from gasses convection from outside the hot zone. A portion of the main quartz tube, as well as a second tube oriented vertically were used to collect ammonium fluoride (NH_4F), and a U-shaped bubble tube was used to monitor the gas flow. The gas inlet configuration allowed to switch between argon (from the software-connected laboratory circuit) and ammonia (from a tank stored inside the fume hood). One filter for ammonia absorption was used at the gas outlet. The full setup is shown in Figure 5.13.

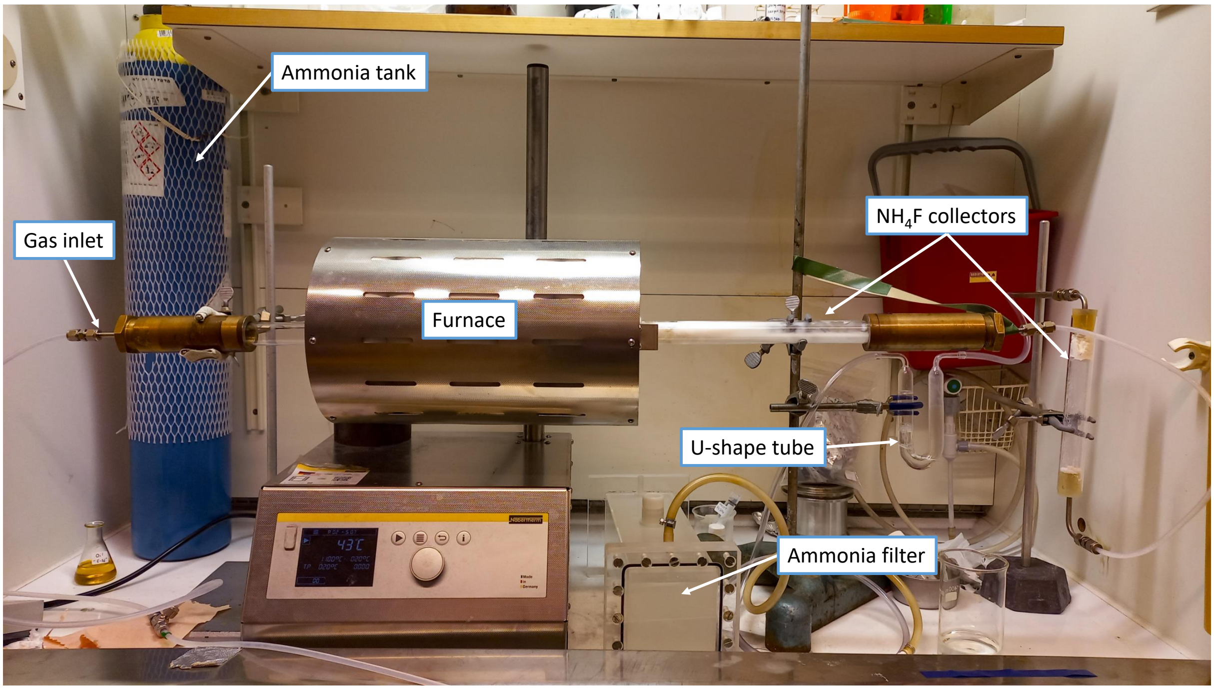

Figure 5.13: Setup for the conversion of the UF_6 products into UN.

5.7.2 Procedure

The procedure was the following:

1. Start the furnace;
2. Start the Ar gas flow (0.15 l/min);
3. Heat from 20°C to 700°C in 68 min (10°C/min ramp);
4. Temperature plateau for 15 min, change the gas to NH_3;
5. Heat from 700°C to 800°C in 100 min (1°C/min ramp);
6. Temperature plateau for 100 min;
7. Change the gas to Ar (0.15 l/min);
8. Heat from 800°C to 1100°C in 30 min (10°C/min);
9. Temperature plateau for 300 min;
10. Let the system cool down in Ar flow.

The tantalum boat was retrieved magnetically and the XRD sample was prepared inside the glove-box, to minimize its contact with air.

5.7.3 Results

NH_4F started to deposit in the main quartz tube cold zone at 240°C in the form of white opacity and as fine dust at 340°C, increasing in amount mainly during the ramp to 700°C. Successively, it started to deposit also as a crusty solid at the furnace outlet and as flakes in the second quartz tube. The uranium product of the reaction was uniformly black but unfortunately, the boat retrieval did not go as planned, and it partially got in contact with air. The XRD analysis results are shown in Figure 5.14 and Table 5.6.

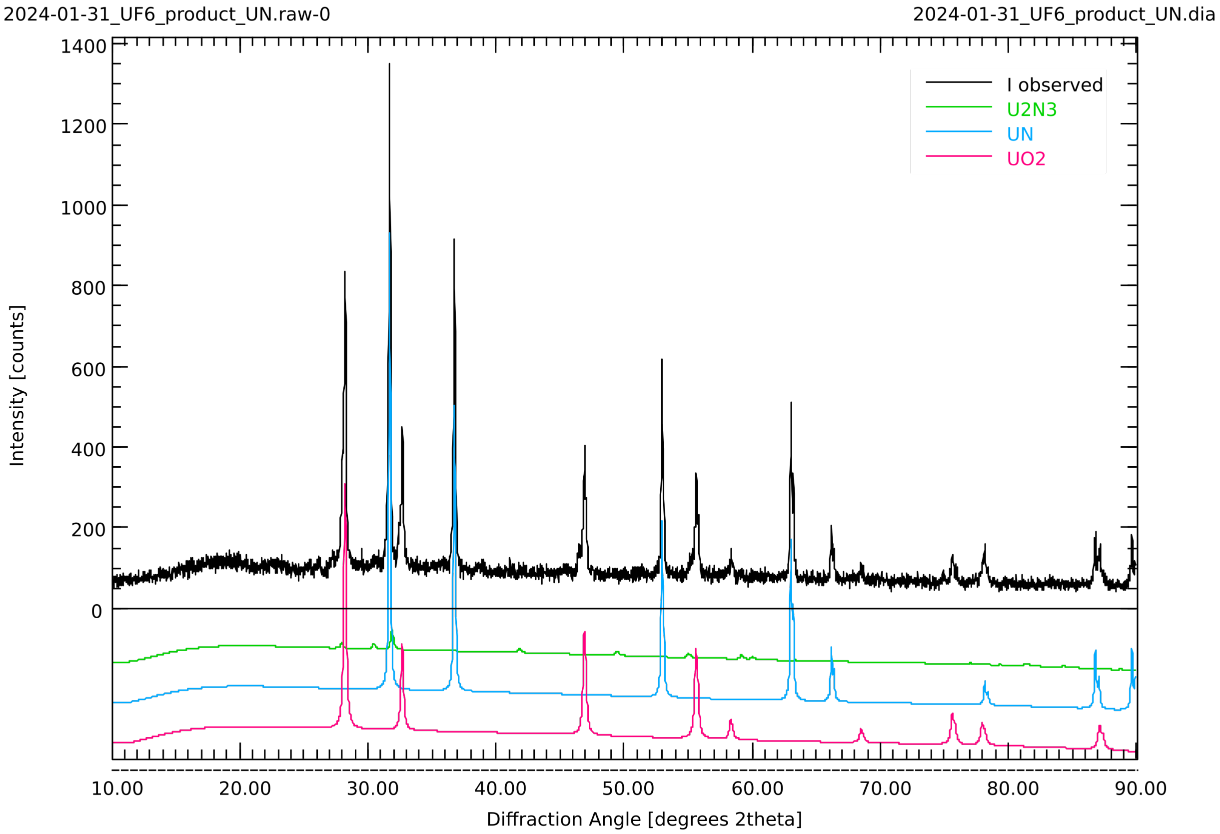

Figure 5.14: XRD pattern of the product of the final conversion to UN.

Table 5.6: Chemical composition of the product of the final conversion to UN*

UN	UO_2	U_2N_3	UN_2
57.5 %	38.9 %	3.2 %	0.4 %

*Phase quantities as reported by the XRD Profex software, the accuracy is low due to counting noise [9].

The experiment was overall a success: even though a little less than half of the product got oxidized during the sample transfer, it proved that the products of different UF_6 ammonolysis experiments could be eventually converted into UN. Future work can aim at achieving UN in a single process from the reaction of UF_6 and NH_3 at 1100°C.

CHAPTER 6

Additional experiments

In addition to the ones described so far, several other experiments have been performed for curiosity and educational purposes. They most relevant to thee topic of this thesis are described in this Chapter.

6.1 Synthesis of UF_4

Based on concepts in publications by Furman and Schoonover [13] and Caley and Rogers [14], a UF_4 synthesis by reduction of uranyl acetate was performed. Zinc was used as reducing agent, according to the following reaction:

$$UO_2{}^{2+} + Zn + 4\,H^+ \longrightarrow U^{4+} + Zn^{2+} + 2\,H_2O$$

For this experiment, the following glassware was used: a conventional flat-bottomed flask, two Erlenmeyer flasks, a 2 µm ultrafilter, and a Bücher funnel equipped with filter paper. Magnetic stirring was used at different stages of the experiment.

6.1.1 Reduction of uranyl acetate

20 ml of 12.1 M hydrochloric acid (HCl) were introduced into 580 ml of deionised water in a flask, in order to obtain a 600 ml 0.4 M HCl solution. 25.1 g of dihydrated uranyl acetate (molar mass 424.146 g/mol) were added, and the flask was placed on the magnetic stirring until the acetate was completely dissolved (Figure 6.1). The resulting solution was light yellow, without any particulates. Since some is consumed by the acid, $4\times$ excess Zinc (molar mass 65.38 g/mol) was used, thus 15.4 g, dumped at once into the solution, which became initially became dark green and later black (Figure 6.2). A cork stopper was placed on the flask neck to minimize oxidation. The flask was left on the magnetic stirrer for 30 minutes to let the reaction happen. Then, it was taken off and the solids (some unreacted Zn) were left to sediment on the bottom of the flask.

Note that the change in color gives evidence that the oxidation state of uranium is reduced from state +6 (yellow) to state +4 (green/black).

Figure 6.1: Solution of uranyl acetate and HCl.

Figure 6.2: Solution after addition of Zn.

6.1.2 Ultrafiltration

The solution was sucked into an evacuated Erlenmeyer flask passing through a polymeric 2 μm ultrafilter, which separated the liquids from the solids (Figure 6.3). The obtained solution was deep dark green.

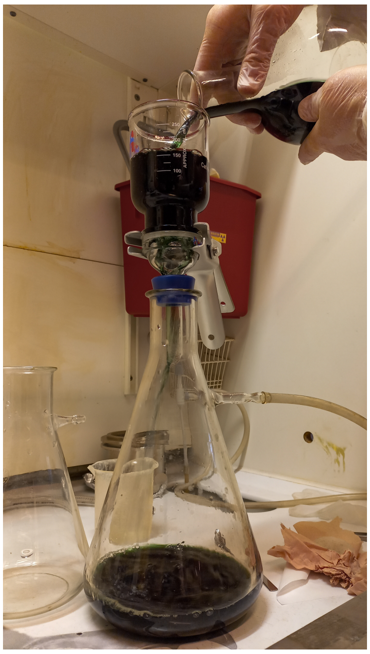

Figure 6.3: Ultrafiltration stage.

Aliquots of concentrated hydrofluoric acid (HF) were added with a pipette: the solution assumed the appearance of a gel, with a layer of liquid on its surface (Figure 6.4).

A filtration station was set up, with a ∅18 cm Büchner funnel equipped with filter paper to retain all solid particles, and an evacuated Erlenmeyer flask containing $CaCl_2$ to render eventual unreacted HF harmless (Figure 6.5).

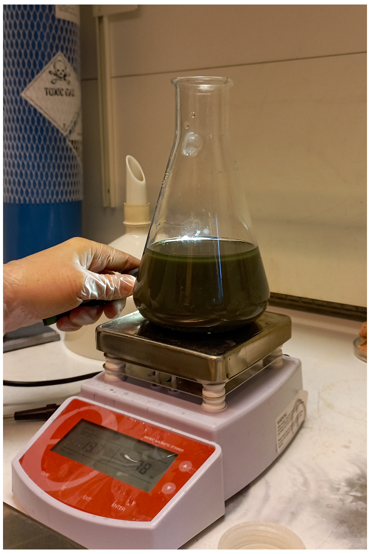

Figure 6.4: Solution after addition of HF.

Figure 6.5: Filtration under suction.

6.1.3 Desiccation

The obtained cake in the funnel was washed twice with pure water and then with acetone, in order to dry it as fast as possible. Figure 6.6 and Figure 6.7 show the product appearance in the funnel and when scraped off from it.

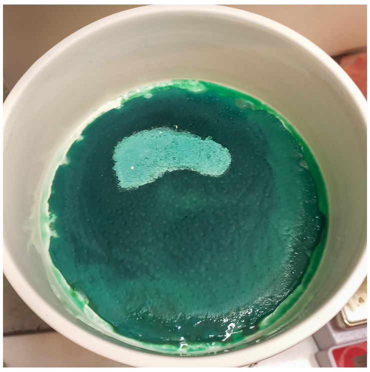

Figure 6.6: Dried product in the funnel.

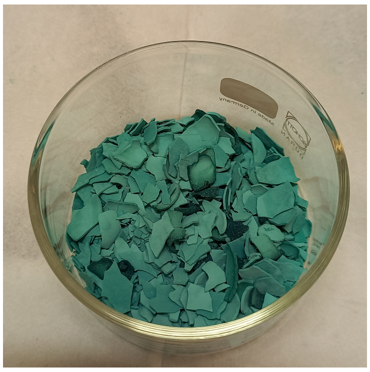

Figure 6.7: Product scraped off from the funnel.

The obtained morphology was particularly interesting in view of an ammonolysis experiment, since the form of big flakes (as opposed to a fine powder) could favor the penetration of ammonia inside the sample bed and could lead to a higher reaction yield.

In order to dry completely, the product was placed over a phosphorus pentoxide (P_2O_5) bad in an evacuated desiccator for more than one month (Figure 6.8).

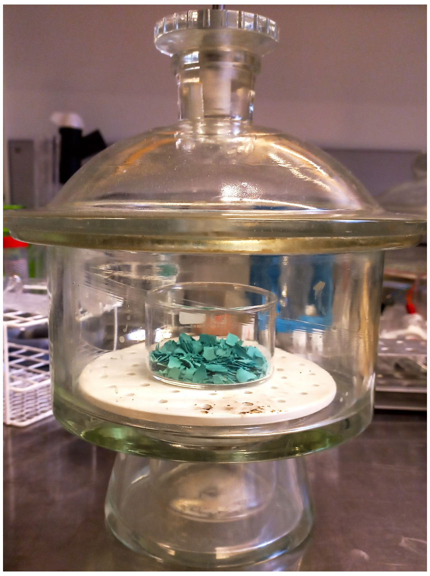

Figure 6.8: Desiccation stage.

XRD analysis was performed to evaluate the quality of the product, and results are shown in Figure 6.9 and Table 6.1. The produced material was indeed UF_4, but more than 75 % of it seemed to fit with the crystallographic data of the hydrated form $UF_4 \cdot 2\,H_2O$. Given the long desiccation time, questions arose about whether water was still truly present in the product or whether the structure was different due to the unconventional production process. A slow desiccation process at room temperature used to remove water from hydrated UF_4 might not lead the structure to spontaneously rearrange into that of UF_4 produced in a ”dry” process. Further investigation is encouraged on this subject, perhaps testing a desiccation process at high temperature and comparing the obtained crystallographic structures.

Table 6.1: Chemical composition of the produced ”Homemade UF_4”*

UF_4	$UF_4 \cdot 2\,H_2O$
24.3 %	75.7 %

*Phase quantities as reported by the XRD Profex software, the accuracy is low due to counting noise [9].

It is important to note that no UF_3 was detected, therefore the reduction was successfully stopped at the UF_4 stage. This is absolutely essential, as UF_3 would not undergo ammonolysis.

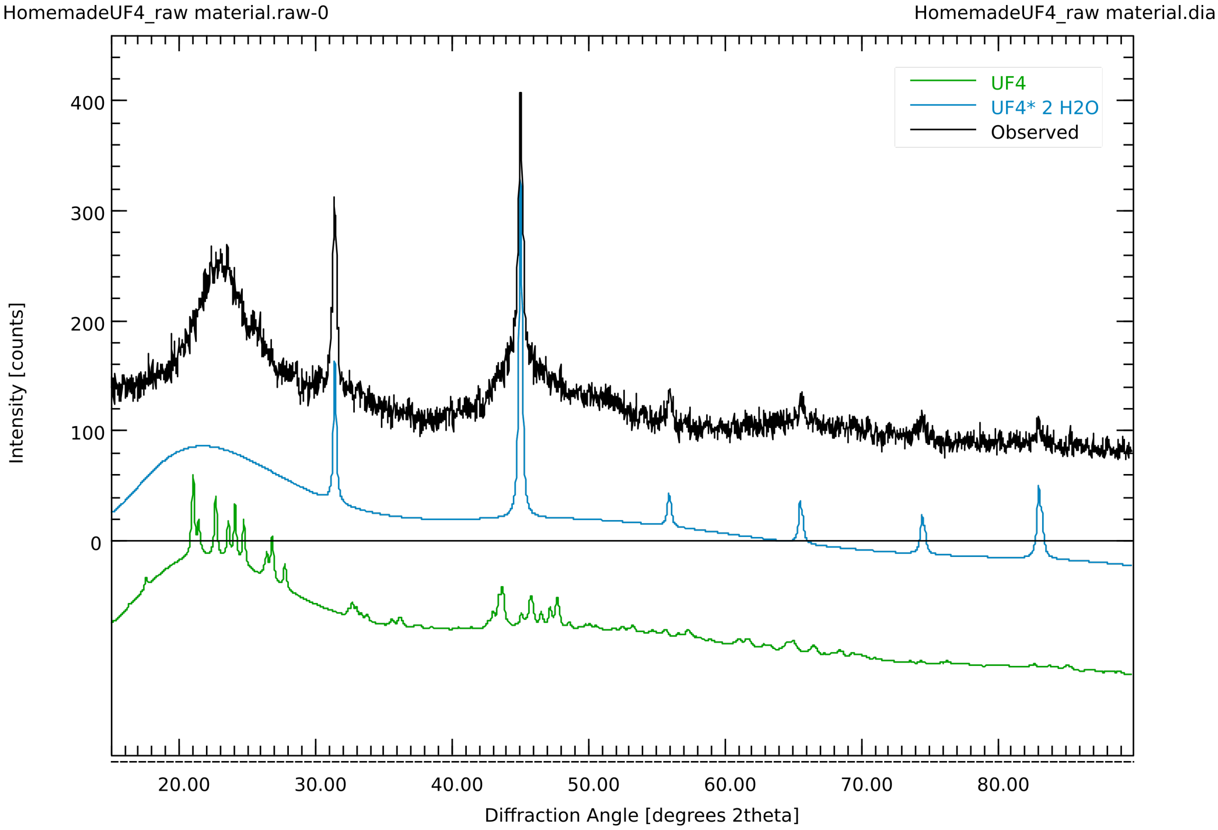

Figure 6.9: XRD pattern of the produced ”Homemade UF_4”.

6.2 ”Homemade UF_4” ammonolysis - small batch

The aim of this experiment was to evaluate the behavior of the ”homemade UF_4” powder in the UN_2 synthesis. The batch used for this experiment was not the one produced during this thesis project, but its composition was very similar (42.7% UF_4, 51.3% $UF_4 \cdot 0.7\,H_2O$). Its evaluation was done by performing an ammonolysis experiment and by investigating the product through XRD analysis.

6.2.1 Setup

During this experiment, heating was provided by the Nabertherm tube furnace (Figure 2.1b), and the reaction was performed inside a quartz tube (1 m, 25 mm ID, 28 mm OD) lined with a 0.3 mm thick copper foil to avoid the formation of water vapor by the reaction of HF with the quartz tube (SiO_2). The sample was chopped, crushed and then placed as a 2-3 mm deep layer in a 100 mm copper boat (Figure 6.10).

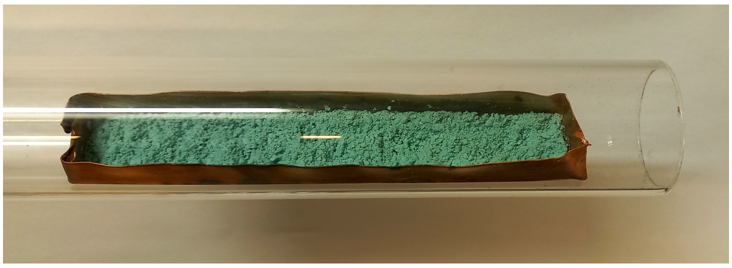

Figure 6.10: UF_4 powder loaded in the copper boat.

Packed copper shavings were used at both ends of the lining to hinder any convection in the tube. Brass fittings supported the tube and avoided its bending during the reaction. A U-shaped bubble tube was placed at the tube outlet and ammonia filters were used in line with it. The complete setup is shown in Figure 6.11.

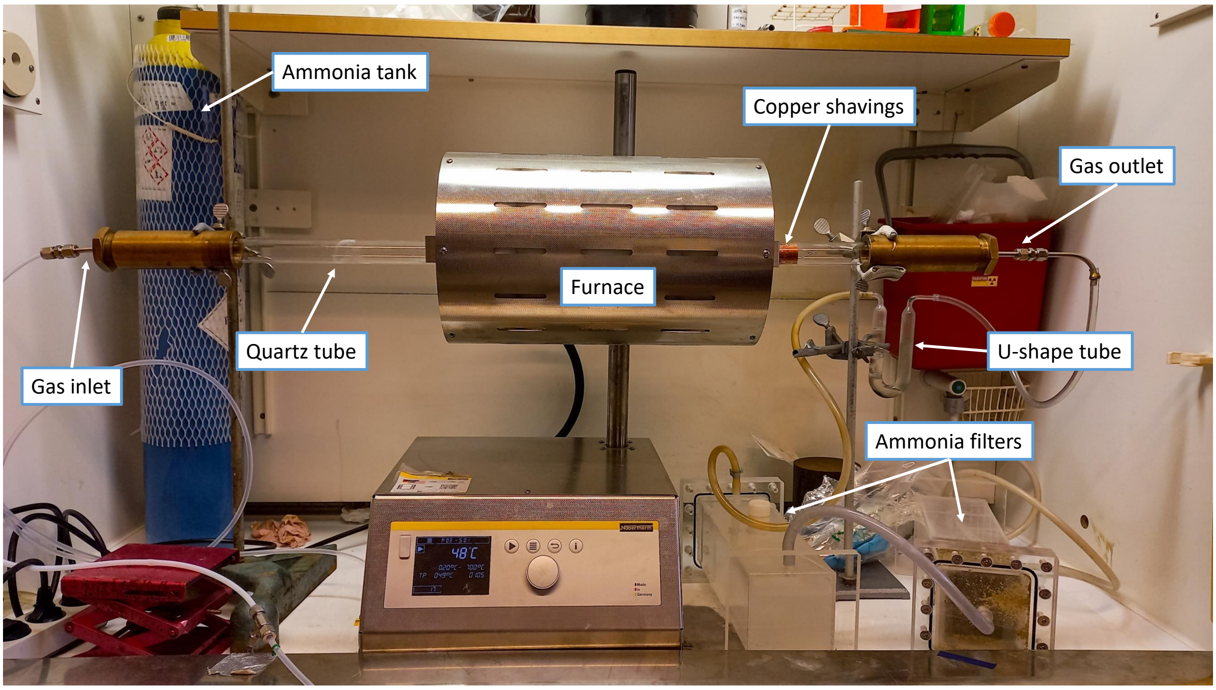

Figure 6.11: "HomemadeUF_4" small batch setup.

6.2.2 Procedure

A 0.2 l/min flow of argon was used to start the experiment. The heating ramp was the following:

- 20 - 700°C: 10°C/min (68 min), the gas was changed to NH_3 at 420°C;
- 700°C plateau for 15 min;
- 700 - 800°C: 1°C/min (100 min);
- 800°C plateau for 100 min;
- 800 - 20°C: 10°C/min (78 min), the gas was changed back to Ar.

The sample was extracted under argon (to avoid oxidation of the product in contact with air) and XRD sample preparation was done in the glovebox.

6.2.3 Results

The experiment was very successful: the first signs of ammonium fluoride were noted at 580°C and formed a translucent deposit on the top part of the quartz tube (hot region of the tube). At 650°C, its quantity was increased, and a white powder started to form on the bottom of the tube, which increased in quantity during the whole synthesis. At the end of the 800°C plateau, the quartz tube was completely opaque, and a big heap of loose NH_4F was present after the outer shaving filter. During cooling in NH_3, additional ammonium fluoride was seen forming, indicating that the reaction was probably still taking place. When the boat was extracted from the furnace, it was noted that the original mass of powder had substantially shrunk. No sign of agglomeration was detected, but the product was a fine, completely unsticky black powder. The XRD analysis showed a UN_2 pattern with a very small UO_2 peak, as shown in Figure 6.12. There were no unidentified peaks and all UF_4 had reacted. The XRD Profex software reported the composition shown in Table 6.2.

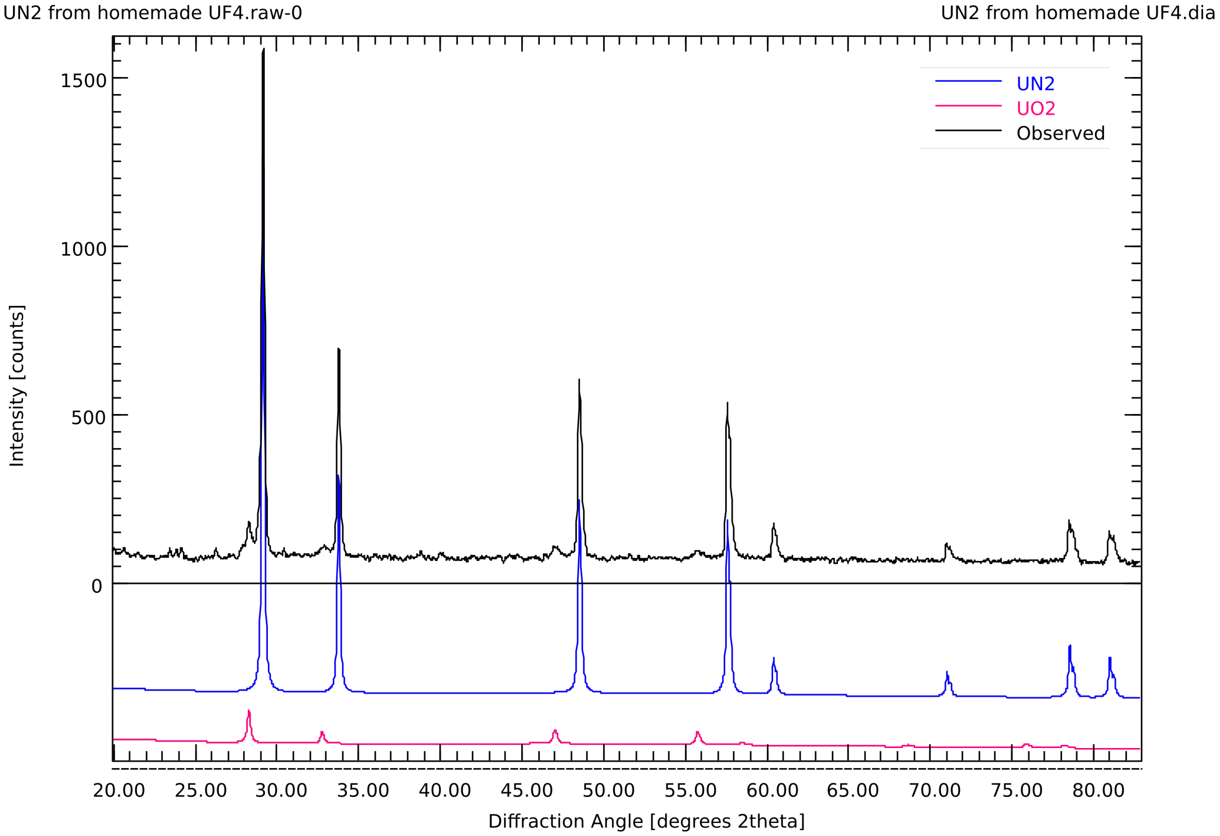

Figure 6.12: XRD pattern of the product of ”homemade UF_4” ammonolysis - small batch.

Table 6.2: Chemical composition of the product of ”homemade UF_4” ammonolysis - small batch*

UN_2	UO_2	UF_4
91.7 %	8.3 %	0.0 %

*Phase quantities as reported by the XRD Profex software, the accuracy is low due to counting noise [9].

The mass balance before and after the reaction reflected the theoretical weight loss quite accurately: before the synthesis, the sample weight was 0.5452 g and after the synthesis it was 0.371 g, with an additional 0.02494 g hidden in the boat. This resulted in a weight loss of 0.149 g, very close to the expected $(4 \cdot 19 - 28) / (238 + 4 \cdot 19) = 0.153$ g per gram of UF_4.

6.3 ”Homemade UF_4” ammonolysis - large batch

Given the success of the synthesis with a small UF_4 batch, the intention was to test a larger batch of the same ”homemade” powder.

6.3.1 Setup

Unfortunately, the same boat (Figure 6.10) could not contain enough sample, therefore the pressure vessel setup was chosen (as in Section 3.1.1). Only a rotameter was added to the setup, in between the U-shaped tube and the ammonia filters. No gas pressurization was used during this experiment. K-type thermocouples were placed inside the furnace chamber, on the vessel lid, and at the two sides of the outlet valve.

6.3.2 Procedure

Heating of the vessel outlet tube was started with 35 V on the power supply, and it was decreased to 30 and then 25 V when the temperature approached 250°C. When the outlet temperature was around 150°C, the furnace was turned on and a very small flow of ammonia was started. It was later increased to 0.1 l/min and then to the nominal 0.2 l/min when the furnace temperature was 350°C. A very slow ramp in the temperature was used from 700°C to 800°C and then the reaction was left to take place during a 100 min plateau at 800°C. After cooling down in argon flow, the sample was retrieved and the XRD sample was prepared in the glovebox.

6.3.3 Results

Some water deposition on the quartz tube was noticed at low furnace temperatures, which could be associated with the small ammonia flow used at the beginning of the experiment (if the ammonia flow was higher, the partial pressure of water vapor would be smaller and water would not condense). This showed that, even if the UF_4 powder had been dried carefully, it still contained some water (note that the desiccation time of this batch was only 7 days). With the increase in temperature, the water vapor started to disappear and the quartz tube was completely dry at 350°C (furnace temperature). Ammonium fluoride deposition started when the temperature in the furnace chamber was around 680°C and it made the quartz tube completely opaque by the end of the experiment (Figure 6.13).

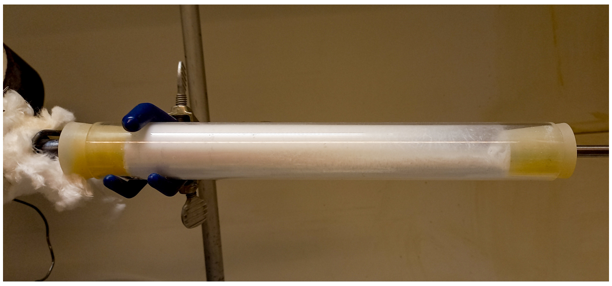

Figure 6.13: NH_4F deposition in the quartz tube from the synthesis of ”homemade” UF_4.

Unfortunately, the XRD analysis was difficult to interpret, since many peaks did not have good matching with any of the known crystallographic structures. The issue was probably the lack of literature regarding the different stoichiometries of uranium sesquinitride (U_2N_3), which was possibly formed during the reaction. However, the observed spectrum was analyzed with the XRD Profex software and results are shown in Figure 6.14 and Table 6.3. Peaks at $2\theta = 26.9°$, $2\theta = 27.7°$ and $2\theta = 45.3°$ remained unidentified.

Table 6.3: Chemical composition of the product of ”homemade UF_4” ammonolysis - large batch*

UF_4	U_2N_3	UN_2	UN	UO_2
49.3 %	16.3 %	15.2 %	6.9 %	5.3 %

*Phase quantities as reported by the XRD Profex software, the accuracy is low due to counting noise [9].

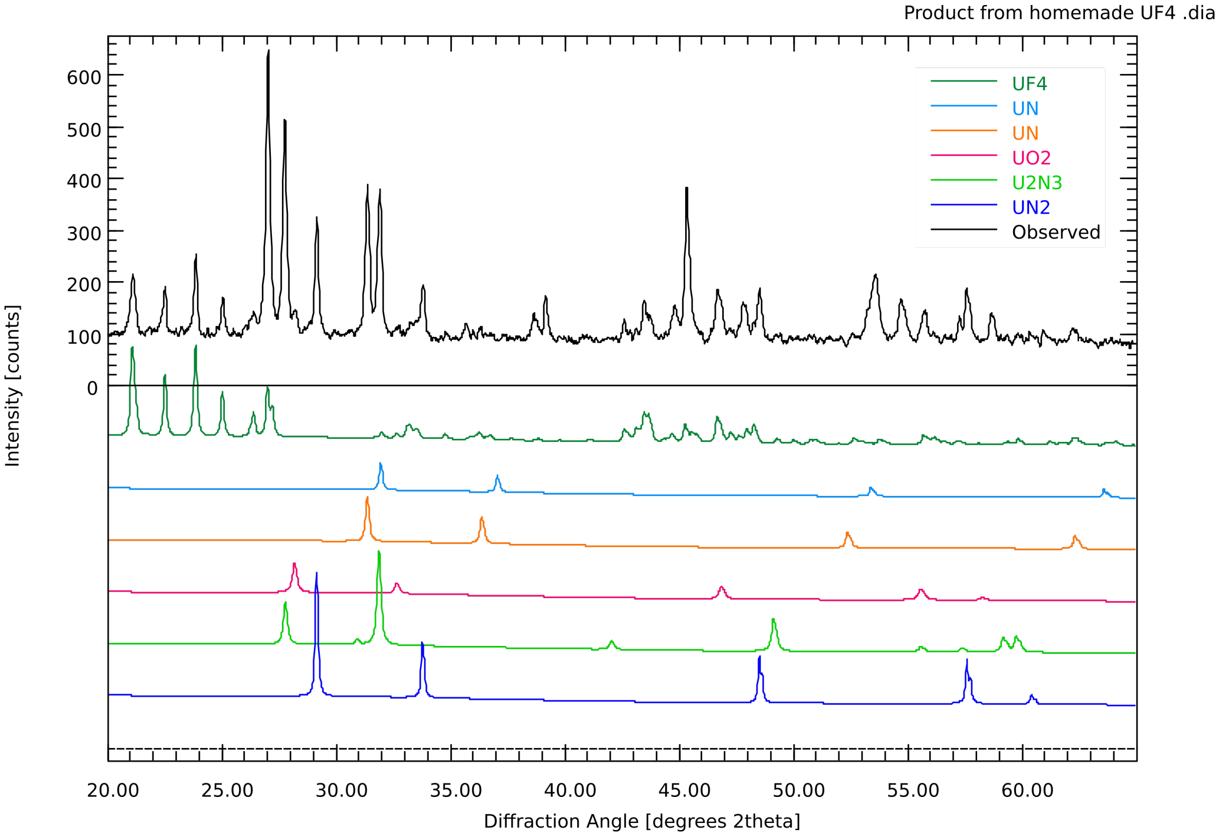

Figure 6.14: XRD pattern of the product of ”homemade UF_4” ammonolysis - large batch.

Despite the not excellent results of this second run, the ”homemade UF_4” production method was successful, as the product seemed to have potential as raw material for the synthesis of UN_2 and successively UN. Moreover, the process is conveniently upscalable, as uranyl acetate can be purchased in large quantities and larger glassware can be used. On the other hand, the setup suitable to perform ammonolysis of a large UF_4 batch still necessitates some improvements.

6.4 Sintering a UN pellet

One of the very few drawbacks of uranium nitride is that it is inherently more difficult to sinter than uranium dioxide: studies have shown that temperatures of 1900 - 2000°C, as well as very long sintering time, are required in a conventional pressureless sintering furnace to achieve 90-95% theoretical density, or 1700°C in case aggressive milling is applied beforehand to produce a sub-micron size UN powder [2]. However, UN pellets with nearly 100% density can be sintered in a few minutes by driving a current of 1000-2000 A through the powder while applying uniaxial pressure, in the so called Spark Plasma Sintering (SPS) method.

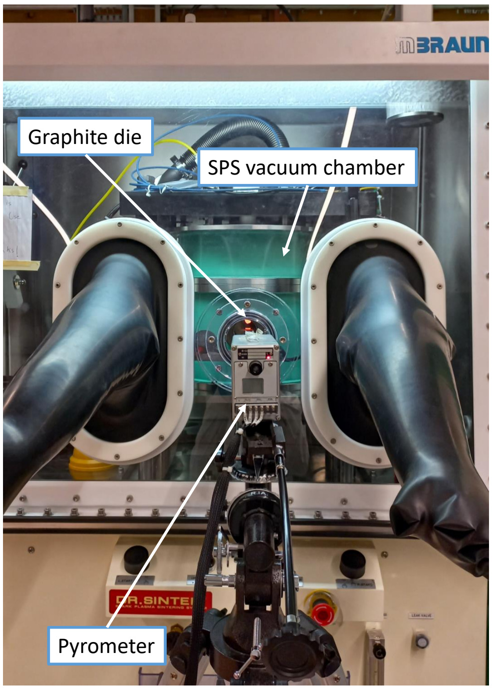

Figure 6.15: Dr. Sinter SPS machine at the national SPS facility (Stockholm University).

During this thesis project, a UN pellet was sintered with the Dr. Sinter SPS-5.40MK-VI at the national SPS facility at Stockholm University, in the Department of Materials and Environmental Chemistry (Figure 6.15). The machine was inside a glove box and operated in vacuum during the sintering process. All procedures of sample preparation were performed in a designated glove box. Approximately 3.5 g of powder was loaded into a 9.3 mm graphite die and pressed between two graphite punches. A thin graphite paper was inserted between the sample and the dies to avoid their direct contact. The assembled die was wrapped into graphite felt insulation to reduce heat losses. Sintering parameters are summarised in Table 6.4.

Table 6.4: Sintering parameters for a UN pellet

Entire sintering time	79 min
Holding time at 1650°C	5 min
Applied uniaxial pressure	80 MPa

The heating rate was set to 100°C/min until 1650°C, which was the target temperature held for 5 min. An optical pyrometer was used to monitor the external temperature of the graphite die. The obtained pellet is shown in Figure 6.16. A 3 mm axial displacement was evaluated by the software connected to the machine in the position of the punches, due to the conversion of the powder into a solid pellet (shrinkage), as shown by the red line in Figure 6.17.

Figure 6.16: UN pellet.

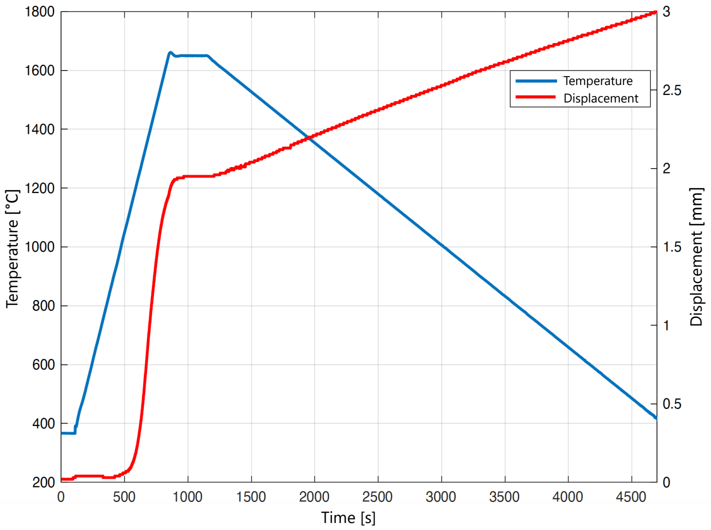

Figure 6.17: Sintering temperature and axial displacement for a UN pellet.

CHAPTER 7

Conclusions

The main objective of this thesis was to develop an innovative method to produce UN by gas/gas reaction of UF_6 and NH_3. To reach this goal, various experiments with UF_4 and UF_6 sources were performed, and vast experience in their ammonolysis was gained.

The intrinsic problem of ammonia dissociation seemed to be the most limiting factor for upscaling, therefore two techniques to hinder it were studied and both gave positive outcomes. In industrial applications, the increase of the gas pressure can potentially eliminate the problem altogether whereas, at the laboratory scale, a pulsed ammonia flow can agitate the powder and expose the unreacted one to the fresh reactant.

Especially in the UF_6 route, the challenge was the use of suitable materials which are, at the same time, not attacked by hydrofluoric acid at high temperatures and not catalytic for the dissociation of ammonia. Copper seems to be suitable for regions below 500°C, while the more expensive tantalum needs to be used in regions at higher temperatures. If the apparatus is constructed from steel or nickel alloys, any hot area not lined with these materials leads to the dissociation of ammonia and reduces the reaction yield.

Concerning the injection of UF_6 in the reaction chamber, two designs have been tested with partial success. Further investigation would be beneficial, perhaps reducing the diameter of the inert gas component, therefore increasing its speed without diluting the reactants.

The separation of the produced UN from NH_4F was also a point in question, and no successful configurations have been found yet: for future work, it will be of interest to test a setup with a dedicated container located at the bottom of the reaction chamber tube, heated at 300°C (to avoid condensation of NH_4F), with large cross-section (to reduce the flow rate and facilitate the deposition of solid particles), and easily movable to the glove box in order to retrieve the product in an oxygen-free atmosphere.

Handling UF_6 in a safe and controlled way was a controversial question at the beginning of this work, but it can be eventually stated that, with appropriate safety measures and with knowledge of the transformations that this material can undergo, it is indeed possible to maintain high levels of safety throughout the whole process.

Future work will essentially aim at the design and construction of a completely oxygen-free setup, where a continuous process from the UF_6 evaporation, through its reaction with NH_3, to the collection of UN can take place. Ultimately, the goal is to upscale the process and operate this methodology at the industrial level.

References

[1] Smith C.F., Cinotti L. *Handbook of Generation IV Nuclear Reactors (Second Edition), Chapter 6 - Lead-cooled Fast Reactors (LFRs)*. Woodhead Publishing, 2023.

[2] Wallenius, J. *Nuclear fuel technologies for liquid metal cooled fast reactors (LMFRs), Chapter 4: Nitrides*. KTH, Division of Nuclear Engineering, Albanova University Centre, Stockholm, Sweden.

[3] *Depleted UF6 Management Information Network Web Site, U.S. Department of Energy*. `http://web.ead.anl.gov/uranium/`. Accessed: 2024-01-22.

[4] *Uranium Hexafluoride: A Manual of Good Handling Practices*. United States Enrichment Corporation, 1995.

[5] Zagoraios, G. *Master thesis: Synthesis of uranium nitride fuel from UF4 stock*. KTH Royal Institute of Technology, Stockholm, 2022.

[6] Grosse, A.V. *Chemical properties of uranium hexafluoride, UF_6*. Department of Physics and Chemistry, Columbia University, New York, 1941.

[7] Döbelin N., Kleeberg R. *Profex: a graphical user interface for the Rietveld refinement program BGMN*. Version 5.2.2. URL: `https://www.profex-xrd.org/`.

[8] *QGA*. `https://www.hidenanalytical.com/products/gas-analysis/qga/`. Accessed: 2023-09-22.

[9] Döbelin, N. *Profex User Manual, Version 4.3*. Solothurn, Switzerland, 2021.

[10] Kurita, C. H. *D-ZERO COLD VALUE*. 1988.

[11] *C 1346 – 08 Standard Practice for dissolution of UF_6 from P-10 Tubes*. ASTM International, 2009.

[12] Galkin N.P. Sudarikov B.N., Zaitsev V.A. *Methods of reducing uranium hexafluoride*. The Soviet Journal of Atomic Energy, 1961.

[13] Furman N.H., Schoonover C. *The indirect volumetric determination of sodium based on the reduction and titration of the uranium in magnesium sodium uranyl acetate*. Journal of the American Chemical Society, 1931.

[14] Caley E.R., Rogers L.B. *Behavior of Uranyl Solutions in a Mercury Reductor*. Journal of the American Chemical Society, 1946.

Appendix

Reactions of UF_6 with water

UF_6 reacts rapidly with water vapor according to the following reactions, releasing large amounts of heat.

- Gaseous UF_6 at high temperatures:

  $$UF_{6(g)} + 2\,H_2O_{(v)} \longrightarrow UO_2F_{2(s)} + 4\,HF_{(g)} + \text{heat} \tag{1}$$

  releases 124 BTUs per pound of UF_6.

- Gaseous UF_6 at room temperature:

  $$UF_{6(g)} + (2 + 4\,x)H_2O_{(v)} \longrightarrow UO_2F_2 \cdot 2\,H_2O_{(s)} + 4\,HF \cdot xH_2O_{(fog)} + \text{heat} \tag{2}$$

  releases 1057 BTUs per pound of UF_6.

- Solid UF_6 with liquid water:

  $$UF_{6(s)} + 1602\,H_2O_{(l)} \longrightarrow UO_2F_{2(aq)} + \text{heat} \tag{3}$$

  releases 258 BTUs per pound of solid UF_6 [4].

Physical properties of UF_6

Table 1: Physical properties of UF_6 [4].

Sublimation point	101 kPa, 56.6°C
Triple point	152 kPa, 64.1°C
Critical pressure	4610 kPa
Critical temperature	230.2°C
Specific heat, solid (27°C)	477 J/kg/K
Specific heat, liquid (72°C)	544 J/kg/K

UF_6 phase diagram

In situations in which UF_6 is in a leak-tight container and it is not visible to the operator, the phase diagram is used to know its physical state as a function of pressure and temperature, so that changes in pressures or weights can be followed.

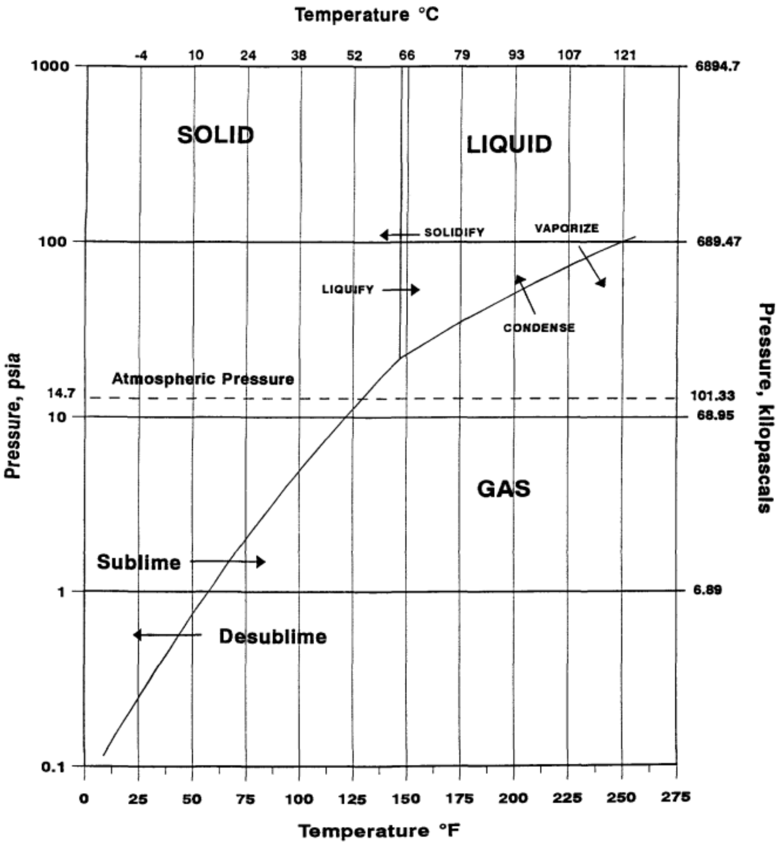

Figure 1: UF_6 phase diagram [4].

Summary of physical properties of uranium compounds

Table 2: Physical properties of uranium compounds [3]

Compound	Melting point [°C]	Density [g/cm^3]	Solubility in water at RT
UF_6	64.1	4.6	decomposes to UO_2F_2
UF_4	960	2.0 - 4.5*	slightly soluble
U_3O_8	Decomposes to UO_2 at 1300	1.5 - 4.0*	insoluble
UO_2	2878	2.0 - 5.0*	insoluble
Uranium metal	1132	19	insoluble

* densities of UF_4, U_3O_8, and UO_2 are highly variable, depending on the production process and the properties of the starting uranium compounds.